Published in final edited form as:
*Thalamus Relat Syst*. 2005 June 1; 3(2): 89–113. doi:10.1017/S1472928805000105.

# Postnatal maturational properties of rat parafascicular thalamic neurons recorded *in vitro*

**K.D. PHELAN**, **H.R. MAHLER**, **T. DEERE**, **C.B. CROSS**, **C. GOOD**, and **E. GARCIA-RILL**
*Center for Translational Neuroscience, Dept of Neurobiology and Developmental Sciences, University of Arkansas for Medical Sciences*

## Abstract

Thalamic relay neurons have homogeneous, adult-like firing properties and similar morphology by 12 days postnatally (PN 12). Parafascicular (Pf) neurons have a different morphology compared with typical thalamic relay neurons, but the development of their electrophysiological properties is not well studied. Intracellular recordings in PN 12–50 Pf neurons revealed several heterogeneous firing patterns different from those in thalamic relay neurons. Two types of cells were identified: Type I cells displayed a fast afterhyperpolarization (AHP) followed by a large-amplitude, slow AHP; whereas Type II cells had only a fast AHP. These cell types had overlapping membrane properties but differences in excitability. Some properties of Pf neurons were adult-like by PN 12, but, unlike thalamic relay neurons, there were significant maturational changes thereafter, including decreased action potential (AP) duration, increased fast AHP amplitude and increased excitability. Pf neurons did not exhibit rhythmic bursting and generally lacked low-threshold spike (LTS) responses that characterize thalamic relay neurons. Pf neurons exhibited nonlinear I–V relationships, and only a third of the cells expressed the time and voltage-dependent hyperpolarization activated (Ih) current, which declined with age. These results indicate that the morphological differences between Pf neurons and typical thalamic relay neurons are paralleled by electrophysiological differences, and that Pf membrane properties change during postnatal development.

### Keywords

development; parafascicular; pedunculopontine nucleus

## INTRODUCTION

The intralaminar thalamic nuclei are a collection of midline cells that have long been considered the ‘non-specific’ arousal portion of the thalamus, based on their extensive input from the ascending reticular activating system (RAS) and their diffuse projection to layer I in the cerebral cortex (Jones, 1985). Classical anatomical studies established the presence of massive projections from the reticular core to both rostral intralaminar nuclei, namely centrolateral (CL)-paracentral (PC), and to the caudal intralaminar nuclei, namely parafascicular (Pf)-centromedial (CM) regions (Pare *et al.*, 1988). The pathway from the reticular core through the CL-PC conveys midbrain reticular efferents presumably involved in synchronization of fast rhythms during waking and rapid eye movement (REM) sleep to many areas of cortex (Steriade and Glenn, 1982). This projection pattern differentiates these thalamic regions from

Correspondence should be addressed to: Edgar Garcia-Rill, Ph.D., Director, Center for Translational Neuroscience, Dept of Neurobiology and Developmental Sciences, Slot 847, College of Medicine, University of Arkansas for Medical Sciences, 4301 West Markham St, Little Rock, AR 72205–7199, USA, email: garciarilledgar@uams.edu.
**Corresponding author**: E. Garcia-Rill, Email: garciarilledgar@uams.edu

the 'specific' projections of the thalamocortical relay nuclei that project to deeper layers of the cortex. However, recent data indicates that individual intrathalamic nuclei have disparate efferent projections, indicating the existence of more specificity within this system than thought previously (Bentivoglio *et al*., 1991; Jones, 2002). In addition, many of the neurons in these nuclei also project to subcortical targets including the striatum (Steriade and Glenn, 1982; Jones, 1985; Sadikot *et al.*, 1990; Sadikot *et al.*, 1992; Bentivoglio *et al.*, 1991; Lai *et al.*, 2000; Jones, 2002; Van der Werf *et al*., 2002). The functional heterogeneity in the intralaminar thalamic nuclei is paralleled by an intranuclear heterogeneity of morphologically, neurochemically and functionally-distinct cell types (Celio, 1990; Frassoni *et al*., 1991; Resibois and Rogers, 1992; Arai *et al.*, 1994; Anna *et al*., 1999; Guillazo-Blanch *et al.*, 1999; Vale-Martinez *et al*., 1999; Harte *et al*., 2000; Hermenegildo *et al*., 2000; Van der Werf *et al*., 2002).

Cells in the 'specific' thalamic nuclei exhibit a similar morphology, regardless of the species or nucleus, which includes radiating primary dendrites with compact bushy dendritic trees (Fig. 1B). These cells also exhibit a stereotypic discharge pattern that depends on membrane potential. A 'tonic' mode of continuous action potential firing occurs when cells are depolarized from an already relatively depolarized membrane potential (as occurs during arousal states), whereas a characteristic, rhythmic, slow oscillation (0.5–4 Hz) with low-threshold spike (LTS) 'burst' mode of firing occurs, especially when they are depolarized from a relatively hyperpolarized membrane potential (as occurs during drowsiness/slow wave sleep) (McCormick and Bal, 1997;Steriade, 1999). Interactions between two voltage-dependent currents, the hyperpolarization-activated cation current (Ih) and the low-threshold calcium current (It) underlie the oscillatory burst mode of firing of these cells (Llinas, 1980). Computational modeling studies indicate that slight changes in either the amplitude or the voltage-dependence of these currents renders thalamic neurons incapable of generating the rhythmic LTS spikes that underlie the slow membrane oscillations (McCormick and Huguenard, 1992;Destexhe and Babloyantz, 1993;Destexhe *et al*., 1993a;Destexhe *et al.*, 1993b;Destexhe *et al.*, 1998;Vasilyev and Barish, 2002). Typically, thalamic neurons exhibit adult-like firing properties and similar morphology by 12 days postnatally (PN 12) (Warren and Jones, 1997).

In contrast, anatomical studies have long recognized that many cells in the Pf have a distinct morphology compared with thalamic relay nuclei (Hazlett *et al*., 1976; Hazlett and Hazlett, 1977; Pearson *et al.*, 1984; Parent and Parent, 2005). Typically, they contain long unbranching processes in their proximal dendritic trees. Because it has been assumed that the electrophysiological properties of Pf and thalamic relay cells are similar, despite these morphological differences, a comparable understanding of the firing patterns of intralaminar neurons is lacking.

## OBJECTIVE

Given that Pf neurons are morphologically different from thalamic relay neurons, this study was designed to systematically explore the questions of whether Pf neurons as a class have different membrane properties, and whether there are significant developmental changes in the electrophysiological properties of Pf neurons beyond PN 12. Therefore, the ages studied (days 12–50) began when thalamic relay neurons are thought to be mature (PN 12) and coincided with, and extended beyond, the well-described period of developmental decrease in REM sleep in the rodent (10–30 days of age) beyond which an adult-like REM sleep pattern is established (Jouvet-Mounier *et al.*, 1970). We used parasagittal-slice preparations that allowed us to record reliably from stable Pf neurons during early postnatal development. An oblique orientation of this slice further enabled us to examine the ascending projections from the PPN to the intralaminar thalamus. We previously reported on the ability of high-frequency stimulation of

PPN to induce prolonged responses in CL and Pf neurons (Kobayashi *et al.*, 2004b). In the present study, we report the heterogeneity of electrophysiological properties of developing Pf cells. We identified two types of Pf cells whose characteristics endured throughout development, and describe several important developmental changes in intrinsic membrane and firing properties that underlie the developmental increase in excitability that occurs in these cells during the period studied. The identification of cell types within the intralaminar thalamus that have intrinsic membrane properties that differ from classic thalamocortical relay cells is a starting point from which to begin understanding the circuitry and function of this region in general arousal and attention. It might also help our understanding of how the loss of Pf cells in Alzheimer's (Rub *et al.*, 2002) and Parkinson's (Henderson *et al.*, 2000) diseases might contribute to altered thalamic function. A preliminary report of some of these findings has been published in abstract form (Phelan *et al.*, 2002).

## METHODS

### Slice preparation

Parasagittal slices of the rat thalamus were prepared from developing Sprague-Dawley rats ranging in age from 12–50 PN ($n = 80$). The animals were anesthetized with ketamine (60 mg $kg^{-1}$, I.M.) until tail-pinch and corneal reflexes were absent, and then rapidly decapitated. The brains were removed from the skull, hand blocked in cooled (4°C), oxygenated (95% $O_2$:5% $CO_2$) artificial cerebrospinal fluid (aCSF) and glued to the stage of a Vibraslice (Campden Instruments). Parasagittal slices were cut at a thickness of 500 μm and allowed to equilibrate at room temperature in oxygenated aCSF for at least 1 hour before recording. Individual slices were transferred to a recording chamber where they were held submerged on a nylon mesh and superfused continuously with oxygenated aCSF at 30–32°C. The gravity-fed flow of aCSF was adjusted to 1–3 ml $min^{-1}$. The aCSF consisted of (in mM): NaCl 122.8, KCl 5, $CaCl_2$ 2.5, $MgCl_2$ 1.2, $NaH_2PO_4$ 1.2, $NaHCO_3$ 26 and D-glucose 10. In some cells, the Ih channel blocker ZD-7288 was dissolved in aCSF at a final concentration of 30 μM and superfused into the recording chamber. In some cases, the slices were prepared in an oblique parasagittal plane that included the pedunculopontine nucleus (PPN), a major source of efferent RAS projections, to examine ascending inputs to the Pf.

### Intracellular recording

Standard intracellular current-clamp recordings were obtained using glass micropipettes pulled from borosilicate glass (with filament) on a Sutter PC-84 micropipette puller. The microelectrodes were filled with 3 M potassium acetate and had final resistances of 60–90 MΩ. Signals were amplified with an Axoclamp 2B amplifier (Axon Instruments) and voltages recorded and analyzed off-line using a Power Macintosh G3 computer and Superscope II software (GWI Instruments). Neurons were impaled and allowed to stabilize a few minutes before testing. Only cells with a stable resting membrane potential (RMP) were included in the analysis. The RMP was verified after withdrawal of the electrode and adjusted according to the offset (usually 1–2 mV). A series of depolarizing and hyperpolarizing current steps (0.1–1.0 nA; 300 ms) were applied in the bridge mode to determine intrinsic membrane properties of Pf cells [i.e. RMP, input resistance (Rin) and membrane time constant]. Current–voltage (I–V) relationships were obtained by holding cells just below the threshold for firing. The properties of action potentials (APs) were analyzed using isolated APs elicited by threshold depolarizing pulses. The expression of putative voltage-dependent currents (such as the transient potassium (Ia), the hyperpolarization-activated (Ih) and the transient calcium (It) current underlying LTS spikes) were determined from the I–V relationships as well as comparisons of responses obtained at holding potentials of −60 mV and −80 mV. Longer duration hyperpolarizing current pulses (up to 600 ms) were tested routinely but failed to reveal differences compared with the standard 300 ms test pulses. In this study, we only considered

a cell to express the Ih current when at least three hyperpolarizing steps elicited a time-dependent sag in the voltage recording and at least one of these was 2 mV or more in amplitude.

### Stimulation of the PPN

In the parasagittal oblique slices, concentric bipolar tungsten stimulating electrodes were placed in the PPN and varying voltages (10–80 V) applied singly or at 10–90 Hz for 1–3 seconds. Synaptic responses were identified by their graded response to increasing voltage application.

### Biocytin injections

Biocytin (1%) was included in some of the recording electrodes to inject Pf cells and confirm recording location, general cell morphology and somatodendritic integrity. The cells were injected with biocytin at the end of the recording session by passing 500-ms depolarizing pulses (~0.5–1.0 nA) at a frequency of 1 Hz for 5–10 minutes. Slices were then removed from the recording chamber and immersion fixed in 4% paraformaldehyde in phosphate buffer overnight. The slices were reglued to the cutting stage of a Vibraslice and serially sectioned into 50–60-μm thick sections. The sections were then processed for biocytin visualization using avidin–biotin histochemistry (Kawaguchi, 1993).

### Statistical analysis

All measurements are reported as mean ± s.e.m. Student's *t*-test was used to compare a single property of two cell groups. Comparisons of properties between different age groups and cell types were assessed for statistical significance using one way analysis of variance (ANOVA) with the Bonferroni post-hoc test. Statistical differences in variances were determined using the F-test. All differences were considered significant at $P < 0.05$, regardless of the statistical procedure. Developmental trends in data and correlations between different sets of data were analyzed using regression slopes and corresponding $R^2$ values.

## RESULTS

Parasagittal brain slices were used to record a total of 181 Pf cells ranging in age from PN 12 to PN 50, although 90% of the cells ($n = 163$) were recorded during the developmental decrease in REM sleep (12–30 days). The primary recording site was restricted to a region caudal to the fasciculus retroflexus (FR) within the area constituting the anterior two-thirds of the area between the FR and the rostral part of the medial medullary lamina (see dotted outline in Fig. 1A). Six cells immediately anterior to the FR displayed identical properties to the more caudally located cells, and were grouped together with the remaining cells for analysis. In our parasagittally cut slices, this caudal region of Pf represents 'medial Pf', whereas in the parasagittal oblique-oriented slices this region encroaches on 'lateral Pf'. In rodents, the medial and lateral parts of Pf are generally considered the equivalents of the primate Pf and CM nuclei, respectively (Jones, 1985). An approximately equal number of Pf neurons were sampled in each type of slice preparation. There was no apparent difference between these cells, therefore, they were pooled for analysis. Stimulation of the PPN resulted in orthodromic excitatory (EPSP) and, less often, inhibitory (IPSP) postsynaptic potentials in Pf cells. High-frequency stimulation of PPN resulted in a prolonged responses in ~20% of Pf cells (11 out of 56 tested), as we reported previously (Kobayashi *et al.*, 2004b) (see also Fig. 13B). Biocytin injections confirmed that the Pf cells recorded in this study exhibited a dendritic-tree branching pattern that was distinct from that of neighboring thalamic relay neurons (Fig. 1B–D). The long, unramifying, primary and secondary dendrites of Pf cells were preferentially oriented parallel to the dorsoventral orientation of the FR. The axons of labeled Pf cells exited the dendritic fields of the cells in a rostral direction and did not appear to give rise to any intrinsic axon

collaterals within Pf, consistent with the projection neuron nature of rat Pf cells. A detailed morphological analysis of Pf cell morphology was not undertaken.

## Differences in AP AHP

Pf cells exhibited a uniform pattern of spontaneous firing consisting of slow irregular firing (~3–5 Hz) when depolarized to firing threshold. However, the population of Pf cells as a whole exhibited heterogeneous intrinsic membrane and firing properties different from the fairly uniform properties of neighboring thalamic neurons. Separate types of Pf neurons did not appear to be defined by specific firing properties. Therefore, for the purposes of description, we defined two types of Pf cell, based on the shape of the AHP following either spontaneous or evoked APs (Fig. 2A). This distinction was paralleled by differences in excitability between these two cell types described below in detail, but was the main enduring characteristic across the developmental period studied. One population of cells (28%, $n = 51$) exhibited a prominent 'notch' between an early fast AHP that immediately followed the AP and a large amplitude slow AHP that peaked later than the fast AHP. We classified these cells as Type I neurons (Fig. 2A, top). The remainder of the Pf cells (72%, $n = 130$) were classified as Type II cells and exhibited APs followed by the initial fast AHP but lacked the later peaking slow AHP (Fig. 2A, bottom). Some Type II cells exhibited evidence of a dual component decay following the fast AHP, but we did not attempt to pharmacologically dissect the various AHP components. The distribution of Type I and Type II cells as a function of postnatal age indicated that this distinction was present at PN 12 and continued throughout postnatal development. Our limited biocytin injections were insufficient to discern any morphological distinction between Type I and Type II cells.

We compared the amplitudes of the fast and slow AHPs in Pf cells as a function of postnatal age (Fig. 2B, C). The mean amplitude of the fast AHP in all cells was 13.7 ± 0.5 mV ($n = 92$). There was no statistically significant difference in the mean amplitude of the fast AHP in Type I versus Type II cells (14.4 ± 0.8 mV and 13.1 ± 0.7 mV, respectively; ANOVA df = 1, F = 1.43). However, a plot of the amplitude of the fast AHPs as a function of postnatal age revealed a developmental increase in the early postnatal period (regression slope, 0.27; $R^2$, 0.16) (Fig. 2B). This appeared to be caused primarily by an increase in the amplitude of the fast AHP in Type I cells (regression slopes were 0.51 versus 0.19 for Type I and Type II cells, respectively). By contrast, the overall mean amplitude of the slow AHP in Type I cells was 15.7 ± 0.8 mV ($n = 36$). There was no comparably clear change in the amplitude of the slow AHP with age (regression slope, 0.03) (Fig. 2C). Although the mean ratio of the amplitude of the two AHPs (fast AHP:slow AHP) in individual Type I cells was 1.01 ± 0.08, two-thirds (23/34) exhibited ratios predominated by larger amplitude slow AHPs. A plot of the fast and slow AHP amplitude ratio in individual Type I cells as a function of postnatal age revealed a shift in this ratio during development (Fig. 2D) (regression slope, 0.03; $R^2$, 0.2). A significant percentage of cells older than PN 20 exhibited a fast AHP that was higher in amplitude than that of the slow AHP.

To better compare the development of these properties, we grouped the early postnatal data into three separate time periods (PN 12–17, PN 18–23 and PN 24–30) (Fig. 2E). These age-groups were chosen because they bracket the period during which there is the most dramatic decrease in REM sleep during development (Jouvet-Mounier *et al.*, 1970). The mean fast:slow AHP amplitude ratio did not differ between cells in the PN 12–17 (0.61 ± 0.12) and PN 18–23 (0.85 ± 0.05) age groups (ANOVA, df = 2, F = 1.6). However, each of these ratios was statistically different from the mean ratio of cells in the PN 24–30 (1.36 ± 0.18) age group (ANOVA, df = 2, F = 7.62; $P < 0.01$ and $P < 0.05$, respectively) because of the shift in direction of the fast AHP:slow AHP amplitude ratio. Further distinctions in the AP properties and excitability of Type I and Type II cells are provided in detail below.

## Intrinsic membrane properties

Table 1 provides the mean values for the intrinsic membrane properties of developing Pf neurons as a whole and as a function of cell type and age. The mean RMP of Pf cells over the entire developmental period studied was −55.2 ± 0.5 mV ($n$ = 172). The mean Rin, measured during the initial linear portion of the I–V relationship, was 107.8 ± 4.3 MΩ ($n$ = 152). The mean membrane time constant measured in response to a 0.3 nA step in current was 9.3 ± 0.5 ms ($n$ = 135). These three intrinsic membrane properties are plotted as a function of postnatal age and cell type in Fig. 3. The distribution of the total population of cells revealed minimal changes in any of these three properties with age. The only significant difference among the three defined age groups was a slight increase in the mean RMP value in the PN 24–30 age group compared with the PN 18–23 age group (ANOVA, df = 2, F = 5.9; $P < 0.01$) (Table 1).

A comparison of these three intrinsic membrane properties in all Type I versus Type II Pf cells indicated no difference in the mean RMP values (ANOVA, df = 1, F = 0.18) (Fig. 3, Table 1). However, there were statistically significant differences in the mean Rin (ANOVA df = 1, F = 4.13; $P < 0.05$) and time-constant values between the two cell types (ANOVA df = 1, F = 6.71; $P < 0.05$). Specifically, Type I cells exhibited higher mean Rin and time constant values compared with Type II cells (~20% and 30% larger, respectively). However, there were significant changes in the RMP values within each cell type in the PN 23–30 age group compared with the PN 17–23 age group. In addition, the time-constant values in Type II cells was significantly different between each of the oldest two defined age groups and the youngest group (ANOVA df = 2, F = 6.8; $P < 0.01$) (Table 1). There were no statistically significant differences in any of these properties between Type I and Type II cells when comparing cells in the three defined age groups individually (Table I). Nevertheless, the mean Rin values of Type II cells were numerically lower than Type I cells in each of the three comparable age groups. Similarly, although the time-constant values of Type I and Type II cells were nearly identical in the PN 12–17 age group, the time constant values in Type II cells were numerically lower in the older two age groups compared with Type I cells.

## Ih current expression

The I–V relationships of developing Pf cells exhibited distinct non-linearities indicative of membrane rectifications (Fig. 4A, B). The most prominent of these was the anomalous time-dependent inward rectifier or Ih current responsible for the slowly developing depolarizing ‘sag’ in the voltage recordings following hyperpolarizing current steps (Fig. 4, open circles). This was evident in 34% of the cells (61/181). The current underlying this voltage deflection was identified as Ih because of its selective blockade with the drug ZD7288 (30 μM, $n$ = 5) (Fig. 4C). The membrane ‘sag’ typically appeared as hyperpolarizations reached membrane potentials greater than −80 mV, although it could be seen in some cells at more depolarized levels. About a third of the Ih cells exhibited only a small amplitude (2–3 mV) change in membrane potential that once present did not vary despite increased membrane hyperpolarization ($n$ = 19). In another third of the cells, the amplitude of the ‘sag’ steadily increased until it reached an initial peak and then did not exhibit an additional voltage-dependent increase in response to further membrane hyperpolarization ($n$ = 20). Some of these cells even exhibited a decrease in Ih amplitude at the most negative hyperpolarizing potentials tested (0.7–0.9 nA currents steps). The remaining third of Ih-expressing cells exhibited a typical pattern of voltage dependency in which the amplitude of the Ih deflection steadily increased as a function of the current step ($n$ = 21).

Examination of the voltage dependence of the Ih in the latter group of cells indicated slopes that ranged from −5–−45 mV $nA^{-1}$ with the overall mean slope of the voltage deflection as a function of current step measuring −17.2 ±2.3 mV $nA^{-1}$ ($n$ = 21). A comparison of these data within the three defined age groups (Fig. 5A) revealed a trend for a developmental decrease in

the mean slope of Ih voltage deflection with a significant decline occurring between the PN 12–17 and PN 18–23 age groups (ANOVA df = 2, F = 6.89, $P < 0.01$). The corresponding mean slope values were −23.9± 4.0 mV $nA^{-1}$ ($n = 9$), −9.5 ± 2.1 mV $nA^{-1}$ ($n = 4$) and −13.1 ± 2.1 mV $nA^{-1}$ ($n = 6$) for the PN 12–17, PN 18–23 and PN 24–30 age groups, respectively.

By contrast, the mean maximal amplitude of the voltage deflection measured at the end of the voltage response to the 0.9 nA hyperpolarizing current step in the entire population of Ih expressing cells was 5.8 ± 0.5 mV ($n = 49$). A plot of the maximal amplitude across age for the entire cell population revealed a regression slope of −0.08, indicating little change in this parameter during postnatal development. The average maximal amplitudes in the three defined age groups were 7.1 ± 0.7 mV ($n = 17$), 4.7 ± 0.8 mV ($n = 19$) and 5.8 ± 1.0 mV ($n = 13$), respectively (Fig. 5B).

Although only a third of Pf cells expressed Ih, Type I cells were more likely to express Ih compared with Type II cells (46% vs 29%, respectively) (Fig. 5C). There was a slight decrease in the percentage of cells expressing Ih as a function of age during the early postnatal period since the linear regression fit of all of the data from PN 12 through PN 50 indicated a slope of −0.69. A plot of the percentage of Ih expressing cells within each cell type as a function of age revealed that this developmental decline primarily reflected a selective decrease in the presence of Ih in Type I cells between the first and second age groups (Fig. 5D).

## Inward rectifying current expression

Almost one third of the Pf cells (27%) displayed a fast voltage-dependent membrane rectification that was distinct from the Ih membrane rectification (Fig. 4A, B, solid circles). This inward rectification appeared as a decrease in the initial peak membrane hyperpolarization with increasing hyperpolarizing current steps, and typically appeared at membrane potentials below −80 mV (Fig. 4B). It was not affected by ZD 7288 (30 μM) at the same time that the drug completely blocked Ih (Fig. 4C). This type of inward rectification could be seen in both Ih and non-Ih expressing cells (Fig. 4). There was a significant difference in the Rin of cells with and without this inward rectification. The average Rin for cells without rectification was 101.8 ± 5.2 MΩ ($n = 102$), whereas the average Rin in rectifying cells measured in the linear part of the I–V relationship before the appearance of the membrane rectification was 122 ± 6.7 MΩ ($n = 46$) (ANOVA df = 1, F = 5.01, $P < 0.05$).

## Types of rebound response patterns

There were differences in the type of rebound response patterns expressed by developing Pf cells in response to the application of a series of 300 ms membrane hyperpolarization current steps of increasing magnitude when held at a membrane potential of −60 mV. We categorized these response patterns into three groups based on the presence of specific cell firing properties (Fig. 6A). The response pattern of these cells did not change when longer duration hyperpolarization pulses were tested. More than one half of the Pf cells (59%, $n = 106$) exhibited either a simple decay back to the baseline, or a partial decay followed by a subsequent low amplitude, long duration membrane hyperpolarization (Fig. 6A, B; see also bottom recording in Fig. 7F). These cells did not exhibit any rebound AP regardless of the amplitude or duration of the hyperpolarizing pulse or changes in holding potential. Another 19% ($n = 34$) of the Pf cells exhibited either a low threshold spike (LTS)-like response (Fig. 6A, B; see also Fig. 9D). These LTS-like responses had amplitudes <20 mV and, typically, only evoked 1 or 2 APs positioned on the rising phase (compared with the large amplitude LTS with multiple APs that can be elicited from neighboring classical thalamic relay neurons) (Fig. 1B). The remainder of the Pf cells (23%, $n = 41$) exhibited a rebound response that consisted of a small amplitude, non-LTS membrane depolarization that included single or multiple APs (Fig. 6A, B; see also Fig. 4C). This rebound spiking persisted at hyper-polarized membrane potentials >−80 mV, at

which Ih channels but not T-channels MIGHT contribute to the spiking since the negative holding potential lies outside of the range of T-channel activation.

Interestingly, Ih-expressing cells were distributed unequally within the three groups. Only 21% ($n$ = 22) of the cells that expressed a decay to baseline with no spiking or LTS-like response were Ih-expressing cells. In contrast, 50% ($n$ = 17) of the LTS-like cells and 54% ($n$ = 22) of the Non-LTS Spiking cells were Ih expressing cells. Nearly 64% ($n$ = 39) of Ih-expressing cells exhibited some sort of rebound depolarizing response compared with ~30% of non-Ih-expressing cells. These data indicate that Ih-expressing cells are more than twice as likely to exhibit rebound spiking than non-Ih-expressing cells, which is consistent with the reported role of residual Ih currents underlying rebound depolarizations. In fact, ZD-7288 reduced non-LTS rebound firing in conjunction with blockade of Ih (Fig. 4C). The majority of the cells in the No Spike group were Type II cells with Type I cells constituting only 19% ($n$ = 20) of these cells. In contrast, Type I cells constituted 38% ($n$ = 13) and 42% ($n$ = 17) of the cell populations in the other two groups of rebound patterns, respectively (Fig. 6A). These numbers are consistent with the overall distribution of Type I cells in the general population.

Each of the three types of rebound response was evident throughout early postnatal development. There was no significant difference in the distribution of these three rebound response types as a function of postnatal age (the mean ages were 22.0 ± 0.9 days, 23.7 ± 1.6 days and 23.0 ± 1.2 days, respectively). A plot of the three rebound response types as a percentage of cells in each of the three defined age groups is shown in Fig. 6C. The percentage of cells expressing a LTS-like rebound response remained relatively stable at 16–18% throughout this time period. In contrast, there was a greater than two-fold increase in the percentage of cells showing the Non-LTS rebound response from an average of 18% for the first two age groups to nearly 38% for the PN 24–30 age group. In addition, there was a concurrent reduction in the percentage of cells in the ‘No Spike’ response group from about 65% to 47% during the same time period. Type I cells appeared to be primarily responsible for this switch.

### Transient potassium (Ia-like) current expression

The transient potassium Ia current contributes to the regulation of AP firing and its presence in neurons is typically reflected as a significant and persistent delay to AP during application of increasing depolarizing current steps. Pf cells had a mean delay to first AP of 71.3 ± 6.8 ms ($n$ = 66) when depolarized from a holding potential of −60 mV (Fig. 7A). The nature of the channel responsible for this Ia-like delay to AP initiation was not tested pharmacologically and is referred to as Ia-like. This delay to AP decreased with increases in depolarizing current steps such that none of the Pf cells had a significant Ia-like induced delay that persisted with increased current steps. There was a statistically significant difference between the delay to AP times in Type I and Type II cells, with Type I cells having twice as long delays (93.8 ± 9.3 ms, $n$ = 34) versus 47.5 ± 8.1 ms, $n$ = 32), respectively) (ANOVA df = 1, F = 13.73, $P < 0.01$). These differences appeared to persist throughout postnatal development (Fig. 7A, B). The duration of the delay to first AP appeared to remain unchanged in Type I cells across the three defined age groups. However, there was a slight decrease in the corresponding values in Type II cells from the PN 12–17 to PN 18–23 age groups (Fig. 7B), although this was not statistically significant (ANOVA df = 2, F = 3.1). In addition to the difference in delay to AP, it typically required higher amplitude current steps to evoke the first AP in Type II compared with Type I cells (0.2 ± 0.02 nA versus 0.15 ± 0.02 nA, respectively) (ANOVA df = 1, F = 4.41, $P < 0.05$). This 40% increase in required current step could have reflected the lower Rin of Type II cells.

The Ia current is also responsible for the significant delay in a rebound AP that follows a hyperpolarizing current pulse since hyperpolarization deinactivates Ia channels, thereby allowing their subsequent activation during the rebound phase of the response. We compared

the delay measured from the end of a 0.5 nA current step application to the return to RMP because this method allowed us to include in our analysis those cells that did not fire an AP during the rebound response. On the basis of the distribution of these values, we identified three populations of neurons indicated by three, non-overlapping, linear regions (Fig. 7C). There was no correlation between the observed delay values and either RMP, Rin or the expression of Ih. Over one half of the cells (51%, $n = 56$) had delays <30 ms with a mean delay of 16.6 ± 1.0 ms and represented cells lacking Ia (Fig. 7C, D). The duration of the delay in this population of cells was positively correlated with the amplitude of the membrane time constant. Nearly one third of the cells (31%, $n = 28$) had delays that fell in the 35–70 ms range with a mean delay of 51.0 ± 1.9 ms, and presumably represented Ia expressing cells (Fig. 7C, D). The remainder of the cells (17%, $n = 11$) had delays of >100 ms with a mean of 234.5 ± 17.2 ms. Most of these cells displayed a long membrane hyperpolarization as part of the rebound response (Fig. 7F). There was no correlation between time constant and the duration of the delay in either of the latter two populations of cells, indicating the presence of an additional voltage-dependent current responsible for the delay. A plot of these three populations as a function of age indicated that all three types were present throughout postnatal development (Fig. 7E). However, the percentage of cells lacking Ia-like delays (<30 ms group) increased from an initial value of 55% in the PN 12–17 age group to 58% and 63% for the older age groups, respectively. There was a corresponding decrease in the percent of cells expressing Ia-like delays (35–70 ms group) from an initial value of 36% in the PN 12–17 age group to 25% and 19% for the PN 18–23 and PN 24–30 age groups, respectively. Finally, the percent of cells exhibiting the long delay increased from 9% in the PN 12–17 age group to 17% and 19% in the PN 18–23 and PN 24–30 age groups, respectively. For cells older than PN 30, there was an obvious decrease in the overall percentage of the cells with the long delay, along with a concomitant increase in the percent of cells with Ia-like delays (now 47%), and a concomitant decrease of cells lacking Ia-like delays to 40%. This suggests that perhaps Ia-like cells are unmasked in some cells during development with the loss of the rebound hyperpolarization.

Comparison of the rebound delay in Type I and Type II cells indicated that, although both cell types contributed to each response pattern, there were developmental differences. The mean delay for the entire population of Type I cells (75.5 ± 16.0 ms; $n = 29$) was 1.7 fold longer than that seen in Type II cells (42.8 ± 6.9 ms; $n = 74$), although this was not statistically significant. The mean delay in the 35–70 ms group of Type I cells (50.0 ± 3.7 ms; $n = 12$) was similar to that in Type II cells (46.7 ± 2.4; $n = 22$).

## AP properties

In addition to the changes in AHPs described previously, Pf cells exhibited significant developmental changes in the properties of APs (Table 2). The mean AP threshold for the entire population of Pf cells was −42.7 ± 0.6 mV ($n = 99$). The mean AP amplitude (measured from AP threshold) was 47.3 ± 0.9 mV ($n = 97$), while the mean AP duration measured at half-amplitude (from AP threshold to AP peak) was 0.93 ± 0.04 ms ($n = 96$). The individual values for these three AP properties are plotted as a function of postnatal age and cell type in Fig. 8. A comparison of the mean values for each of these three AP properties across the three age groups indicated that there was no statistically significant change in the mean AP threshold (combined PN 12–30 regression slope of −0.25, $R^2 = 0.03$) (Fig. 8A). There was a slight increase in the AP amplitude that occurred between the first and third age groups (ANOVA df = 2, F = 4.2, $P < 0.05$) (combined PN 12–30; regression slope, 0.38, $R^2$, 0.04) (Fig. 8B). In addition, a significant decrease in mean AP duration occurred between cells in the PN 12–17 and PN 18–23 age groups but did not decrease further (ANOVA df = 2, F = 29.9, $P < 0.01$) (PN 12–30 regression slope of −0.05, $R^2 = 0.31$) (Fig. 8C). A comparison of these AP properties in the entire population of Type I versus Type II cells indicated no statistically significant difference in any AP parameter between the two cell types (ns) (Table 2). A similar comparison

within the three defined age groups indicated that Type II cells had nearly a 50% longer AP duration compared with Type I cells during the PN 12–17 age group but not in the later age groups (ANOVA, df = 5, F = 15.7, $P < 0.01$). The AP duration declined in both cell types during the PN 12–30 time-period with Type II cells exhibiting the greatest decrease (regression slopes were −0.03 ($R^2$, 0.20) and −0.06 ($R^2$, 0.44). Most of this decrease occurred between the first two defined age groups. Although there were no significant differences in mean AP threshold or amplitude between Type I and Type II cells in any age group, there was a significant increase in AP amplitude between the first and third age groups in Type II cells (ANOVA df = 5, F = 2.53, $P < 0.05$).

## Firing patterns

We identified three main types of firing patterns in Pf cells in response to a series of depolarizing current steps applied from a holding potential of −60 mV (Fig. 9). Although the majority of cells could be classified into one of these three groups (67%, $n = 120$), the remaining cells displayed mixed patterns of firing that likely reflected cells undergoing a developmental transition between firing patterns (see below). A minority of the cells (20%, $n = 24$) fired a single AP at the beginning of the current step and then failed to fire additional APs despite increases in currents step applied (Fig. 9A, B; see also Fig. 10C). Nevertheless, the delay to first AP decreased in these cells with increasing current application. Three-quarters of these single AP-firing cells were Type II cells. Almost a third of the Pf cells (32%, $n = 38$) fired an initial series of APs but then accommodated or ceased firing during the current step (Fig. 9A, B). This AP accommodation pattern persisted at all levels of membrane depolarization. Some of these cells exhibited an initial period of burst-like firing and the later occurring APs often had lower amplitudes and were of longer duration compared with the earliest evoked APs. The majority of these cells were Type II cells (84%) (e.g. Fig. 12). Many of these accommodating cells also displayed a hyperpolarizing membrane rectification during the depolarizing current steps that might have contributed to the AP accommodation. This hyperpolarization typically was ~4 mV in amplitude as measured from the end of AP firing to the end of the current step. The presence of this feature did not appear to be correlated with either postnatal age or cell type, and the cells appeared healthy in all other respects (i.e. RMP, Rin, time constant, AP, etc). This hyperpolarization was not significantly different when the cell was held at −80 mV compared with −60 mV (e.g. Fig. 9C). The third and most common type of firing pattern exhibited by Pf cells (48%, $n = 58$) was a continuous train of APs with the number of APs increasing as a function of current step (Fig. 9A, B). Over one half of these repetitively firing cells were Type I cells (53%, $n = 31$) (e.g. Fig. 11). Many of the cells fired a burst of APs during the initial part of the response and then attained a plateau rate of firing. Those cells which could not be easily be categorized in one of these three groups often displayed a predominant pattern of decrementing or repetitive spike firing at the initial depolarizing current steps but changed their firing pattern at more depolarizing steps.

A plot of the distribution of these three distinct firing patterns as a function of developmental age indicated that all three types of firing patterns could be found throughout the developmental period studied (Fig. 9C). However, there was a clear developmental decline in the overall percentage of single AP-firing cells during early postnatal development with a concomitant increase in the percentage of repetitive firing cells. Early in development (PN 12–17 age group), Type II cells were nearly as likely to display any of the three firing patterns, while the majority of Type I cells displayed the accommodating firing pattern. Later in development (PN 24–30 age group), the firing patterns of the majority of the Type I and Type II cells segregated into the repetitive and accommodating patterns, respectively (Fig. 9C).

### Voltage-dependent firing patterns of Pf cells

One prominent characteristic of classical thalamic relay neurons is the voltage-dependent change in the firing pattern of cells from a repetitive firing mode to a LTS burst firing mode as the cells are hyperpolarized. A comparison of the firing properties of Pf cells at −60 mV and −80 mV indicated that the majority of cells failed to display significant changes in firing properties. None of the cells displayed rhythmic LTS-like burst firing, such as that underlying slow oscillations in thalamic neurons triggered by hyperpolarizing current pulses or occurring spontaneously (Steriade *et al.*, 1993), at any membrane potential. The slow membrane oscillations that are common in thalamic relay neurons (Steriade *et al.*, 1993) were present in only a few Pf cells (Fig. 10). Representative recordings from a repetitive firing and an accommodating cell are shown in Fig. 12 and Fig. 13, respectively. In each example, although the rate of AP firing decreased with comparable current steps after membrane hyperpolarization, the overall pattern of repetitive and accommodating AP firing was not altered significantly by changes in the holding potential. In some cells, a relatively small amplitude LTS-like response (Fig. 12B, arrow) was apparent at −80 mV but not at −60 mV during depolarizing steps. This LTS-like response appeared to underlie the generation of 2–4 APs during the initial part of the depolarization especially at more depolarized current steps. Interestingly, because these cells typically exhibited a similar burst of high frequency firing during the initial part of the depolarizing response when held at −60 mV, the presence of the LTS-like response at −80 mV did little to change the overall firing pattern.

### Frequency-response profile of Pf cells

The I–V relationship of AP firing of Pf cells revealed that the frequency of firing increased linearly with increasing current step. The frequency response profiles of a repetitively firing Type I and an accommodating Type II cell are shown in Fig. 12 and Fig. 13, respectively. In general, Type I cells had flatter instantaneous frequency-current (f-I) plots compared with the steep f-I plots that characterized Type II cells regardless of whether the cells displayed a repetitive or accommodating firing pattern. An analysis of the instantaneous firing frequency for the first interspike interval (ISI) revealed an average frequency of 24.7 ± 1.2 Hz/0.1 nA ($n$ = 67). A comparison of the instantaneous firing frequency profiles of Type I versus Type II cells is shown in Fig. 11. Type I cells typically exhibited lower firing frequencies (mean 18.6 ± 1.2 Hz/0.1 nA; $n$ = 32) compared with Type II cells (mean 30.5 ± 1.8 Hz/0.1 nA; $n$ = 34) (ANOVA df = 1, F = 30.8, $P < 0.01$) (Fig. 11A). A plot of the mean slope of the instantaneous firing frequency for the first ISI as a function of age revealed a clear developmental increase of AP firing frequency during the early postnatal period (combined regression slope, 0.94; $R^2$, 0.13 for all cells shown in Fig. 11B) ($n$ = 66). The mean slope of Type I versus Type II cells were essentially parallel during this time period [regression slopes of 0.96 ($R^2$, 0.09) versus 1.00 ($R^2$, 0.20), respectively] (Fig. 11B). However, the average slope of Type II cells was shifted to the left compared with Type I cells, which reflects their relatively higher basal firing rate and their shorter duration AHP (Fig. 11B). Analysis of the mean instantaneous firing frequency for all ISIs revealed an average frequency of 15.19 ± 0.95 Hz/0.1 nA ($n$ = 62) for the entire cell population (Fig. 11D). This value was lower than that seen for the first ISI, reflecting the fact that firing frequency decreased during a depolarizing step in all cells examined.

Comparison of the mean instantaneous firing frequency profiles of Type I versus Type II cells as a function of current step exhibited a similar linear relationship as that seen for the first ISI (Fig. 11C). The mean instantaneous firing frequency of Type II cells (16.7 ± 1.5 Hz/0.1 nA, $n$ = 30) was slightly higher than that of Type I cells (13.8 ± 1.1 Hz/0.1 nA, $n$ = 32), although this difference was not statistically significant (ANOVA df, 1; F, 2.5). The mean instantaneous firing frequency as a function of age indicated a similar, although lower, developmental increase of mean firing frequency during the early postnatal period (combined regression slope,

0.48; $R^2$, 0.15 for all cells shown in Fig. 11D). The mean slope of Type I cells was 0.45 ($R^2$, 0.14) whereas the mean slope of Type II cells was 0.55 ($R^2$, 0.18) (PN 12–36) (Fig. 11D). Even steeper regression slopes were evident during the earlier PN 12–24 time period indicating that steady increases occurred in these values during this postnatal period.

Because we previously reported a relationship between Ih expression and cell excitability in the PPN (Kobayashi *et al.*, 2004), we further examined the first ISI and mean ISI firing frequency data to determine the relationship between Ih expression and cell excitability. In each case, cells without Ih exhibited ~50% higher excitability. The mean slope of the instantaneous firing frequency for the first ISI in all Ih expressing cells (26.7 ± 3.0 Hz/0.1 nA, $n = 26$) was significantly lower than that of cells lacking Ih (36.3 ± 2.4 Hz/0.1 nA, $n = 38$) ($P < 0.01$). Measurement of these values as a function of postnatal age indicated that a similar developmental increase in excitability occurred regardless of Ih expression pattern (each regression slope, 0.8; $R^2$, 0.09). Similarly, the mean slope of the instantaneous firing frequency for all ISIs in all cells expressing Ih (12.8 ± 1.1 Hz/0.1 nA, $n = 25$) was significantly lower than that of cells lacking Ih (16.8 ± 1.4 Hz/0.1 nA, $n = 37$) ($P < 0.05$). Although there was a developmental increase in excitability in non-Ih expressing cells (regression slope, 0.61; $R^2$, 0.18), the Ih expressing cells exhibited significantly less age-dependent increases (regression slope, 0.16; $R^2$, 0.03).

To determine if there was a cell type difference in excitability in Ih expressing cells, we compared the corresponding mean ISI firing frequency values in Type I versus Type II cells. The mean slope of the instantaneous firing frequency for the first ISI in Type I cells with Ih (25.3 ± 4.3 Hz/0.1 nA, $n = 14$) was lower than that seen in Type I cells lacking Ih (33.8 ± 3.9 Hz/0.1 nA, $n = 18$) ($P < 0.05$). Similarly, the mean slope of the instantaneous firing frequency for the first ISI in Type II cells with Ih (28.3 ± 4.3 Hz/0.1 nA, $n = 12$) was also lower than Type II cells without Ih (38.6 ± 2.8 Hz/0.1 nA, $n = 20$) ($P < 0.05$). However, there was no statistically significant difference in these values when comparing Ih expressing or non-expressing cells in the Type I and Type II population of cells (ANOVA, df = 3, F = 2.5, $P > 0.05$). These comparisons indicated a clear developmental increase in excitability (as measured by the instantaneous firing frequency of the first ISI) in each cell type regardless of Ih expression, especially during the initial PN 12–26 time period. The mean slope of the instantaneous firing frequency for all ISIs in Type I cells with Ih (13.3 ± 1.5 Hz/0.1 nA, $n = 14$) was similar to that in Type I cells without Ih (14.1 ± 1.6 Hz/0.1 nA, $n = 18$). However, the mean instantaneous firing frequency for all ISIs in Type II cells without Ih (20.0 ± 2.0 Hz/0.1 nA, $n = 20$) was >50% higher compared with Type II cells with Ih (12.0 ± 1.4 Hz/0.1 nA, $n = 12$) ($P < 0.05$). However, there was no significant difference in these values between Type I and Type II cells regardless of Ih expression pattern ($P > 0.05$). Therefore, these comparisons indicate a clear developmental increase in excitability (as measured by the instantaneous firing frequency of all ISIs) regardless of cell type or Ih expression.

## Depolarization-induced AHPs and afterdepolarizations (ADPs)

A significant population of Pf cells (~25%, $n = 45$) displayed prominent AHPs following the end of depolarizing current steps. In the majority of these cells, the amplitude of this AHP varied as a function of the depolarizing current step with an average amplitude of 5.7 ± 0.4 mV. These cells were nearly twice as likely to be Type I cells compared with Type II cells (62% Type I; 38% Type II). About one half of these cells had an Ih current (53%, $n = 24$), whereas only 24% ($n = 11$) exhibited a LTS-like response.

Fewer Pf cells ($n = 7$) displayed a prominent afterdepolarization (ADP) that followed a short duration AHP at the end of depolarizing current steps (Fig. 14A). The amplitude of this ADP varied as a function of the preceding depolarizing current step and averaged 3.6 ± 2.5 mV and the duration generally lasted several seconds. Typically, the amplitude of the preceding AHP

did not decrease as the amplitude of the ADP increased. Interestingly, all of the cells expressing an ADP were Type I cells older than PN 18. Over 50% expressed a prominent Ih (4/7), but none expressed a LTS. A prolonged response similar to the ADP can be elicited in Pf cells following high frequency stimulation of the PPN (Kobayashi *et al.*, 2004b). In the PN 17 Pf cell in Fig. 14B, high-frequency stimulation of the PPN for 1 sec at 60 Hz induced a prolonged low-amplitude response that elicited APs when stimulation increased to 100 Hz.

## CONCLUSIONS

### Heterogeneity of electrophysiological properties of Pf neurons

We concentrated our recordings on cells in the caudal part of Pf situated immediately posterior to the FR because this region can be identified easily in parasagittal slices. We found no obvious differences between cells in the medial Pf recorded in strict parasagittal slices and those cells encroaching upon the lateral Pf recorded in oblique parasagittal slices. However, we cannot exclude the possibility that there might be subtle differences between the two regions, especially because the lateral Pf in rodents appears to be homologous to the primate CM nucleus (Jones, 1985). Our data indicate heterogeneity in the electrophysiological properties of Pf neurons. For purposes of description, we defined two types of Pf cells that could be distinguished by the type of AHP seen following individual APs. Type I cells exhibited a pronounced two component AHP with an early fast AHP separated from a later slow AHP by a distinct ‘notch’. Type II cells exhibited the fast AHP but lacked the large amplitude slow AHP. These two cell types exhibited considerable overlap in their intrinsic membrane, but each had their own predominant set of cellular characteristics contributing to differences in excitability. They also appeared to differ in maturation because the characteristics of thalamic relay neurons are fairly mature by PN 12, whereas some characteristics of Pf cells kept developing, at least through PN 30.

The morphology of the biocytin-labeled Pf cells sampled in this study matched that previously reported for Pf cells in rodents and other species using various single cell labeling techniques (Hazlett *et al.*, 1976; Sugiyama *et al.*, 1992b; Fenelon *et al.*, 1994; Deschenes *et al.*, 1995; Deschenes *et al.*, 1996; Vercelli *et al.*, 2003; Parent and Parent, 2005). Specifically, Pf cells exhibited long, unramifying primary dendrites unlike the compact, bushy dendritic trees which characterize neighboring thalamic relay neurons in the rat (Harris, 1986; Sawyer *et al.*, 1989; Bartlett and Smith, 1999; Li *et al.*, 2003). We did not conduct a detailed morphological analysis of Pf cells and therefore cannot comment on any potential correlation between electrophysiological and morphological properties in Type I and Type II cells.

From a functional standpoint, is important to determine if the two general Pf cell types identified in this study receive different afferent inputs and/or project to distinct efferent targets. In this regard, previous electrophysiological studies have documented the heterogeneity of cells in the Pf nucleus based on differences in their responsiveness to different sensory afferent inputs (Matsumoto *et al.*, 2001; Minamimoto and Kimura, 2002). A further differentiation between ‘noxious-on’ and ‘noxious-off’ cell types has been reported in rat Pf (Liu *et al.*, 1993). A differential role of specific Pf cell types in nociception might explain how ablation of Pf in humans results in a selective reduction in the emotional (affective) component of pain (Uematsu *et al.*, 1974; Whittle and Jenkinson, 1995; Young *et al.*, 1995a; Young *et al.*, 1995b) whereas high-frequency stimulation of Pf induces intense pain (Sano *et al.*, 1966; Velasco *et al.*, 1998). However, any distinction between the functional role of Type I and Type II Pf cells awaits further characterization of their anatomical connectivity and pharmacological response profile. Furthermore, it is unclear how the two Pf cell types described here correspond to the various Pf cell types defined using extracellular recording methods (Andersen and Dafny, 1983).

## Developmental changes in intrinsic membrane and AP properties

The RMP, Rin and time-constant values of Pf cells as a whole were already established at approximately adult levels by PN 12. There were only minor changes evident in these characteristics during the PN 12–30 period that primarily reflected an apparent decrease in the variances around the means, especially after the first postnatal period studied (PN 12–17). Most of these changes appeared to reflect developmental changes in Type II cells, supporting the fact that Type I neurons appeared to be more developmentally mature than Type II cells. In addition, Type I cells had significantly higher Rin and time constant values compared with Type II cells, which indicates that they may be larger. Moreover, the overall RMP, Rin and time-constant values in Pf cells were not remarkably different than those reported for neurons in thalamic nuclei of other rodents (Avanzini *et al.*, 1989; Hernandez-Cruz and Pape, 1989; Goaillard and Vincent, 1992; Velazquez and Carlen, 1996; Macleod *et al.*, 1997; Warren and Jones, 1997; Perez Tennigkeit *et al.*, 1998; Li *et al.*, 2003) or Pf in adult guinea pig (Jahnsen and Llinas, 1984a; Jahnsen and Llinas, 1984b; Sugiyama *et al.*, 1992a).

In parallel with the modest changes observed in the passive membrane properties of Pf cells, we found substantial developmental changes in AP properties during the developmental period studied. Although the threshold for AP generation did not appear to change significantly in either cell type, there were prominent changes in the AP amplitude and duration, especially in Type II cells. The most significant change was in the mean AP duration of Type II cells, in which the duration was reduced by nearly 50% during PN 12–30 period, with the greatest decline occurring during the first week studied. This developmental decline in AP duration might partly reflect the concomitant increase in the amplitude of the fast AHP that occurred in Pf cells during the same period. These changes in AP properties are likely to contribute to the developmental increase in firing frequency that we observed in Pf cells. It has been reported that, in other thalamic nuclei, these AP properties are relatively adult-like at PN 12–14 (Perez Velazquez and Carlen, 1996; Warren and Jones, 1997; Tennigkeit *et al.*, 1998) but the same properties in mouse lateral geniculate neurons only reach the adult pattern by ~PN 21 (Macleod *et al.*, 1997). Our data, thus, indicate that the development of AP properties in Pf exhibited a significant developmental delay compared with neighboring thalamic nuclei in rodents.

## Developmental changes in firing pattern and frequency

We identified three main AP patterns of firing for Pf cells in response to depolarizing step pulses: single AP firing; repetitive AP firing (non-accommodating); and a decrementing (accommodating) pattern of APs. These three patterns were not restricted to a particular cell type or postnatal age. However, the single AP and decrementing AP patterns were primarily evident in Type II cells, whereas the majority of Type I cells exhibited the repetitive firing pattern. Furthermore, the single AP and decrementing AP patterns were most prominent during the early PN 12–17 time period studied, whereas in the older PN 18–30 time period, the repetitive firing pattern was the dominant pattern and the single AP pattern was greatly reduced. These changes might reflect the maturation of voltage-dependent conductances underlying AP generation and/or a corresponding developmental change in the afferent input to Pf cells. For example, AP-frequency accommodation mediated by calcium-activated potassium conductances can be blocked by activation of different neurotransmitter receptors, including acetylcholine, serotonin, norepinephrine and metabotropic glutamate receptors (Malenka *et al.*, 1986; Andrade and Nicoll, 1987; McCormick *et al.*, 1991; Davies *et al.*, 1995). Developmental changes in neurotransmitter-specific afferent inputs to Pf during this early postnatal period, especially as it relates to modulation of cell firing, remains an unexplored area of research. Regardless of the underlying mechanism for the observed changes in firing patterns, these changes reflect the substantial developmental increase in excitability that Pf cells exhibit during the period sampled.

The majority of Pf cells fired a series of APs during depolarizing current-pulse application and, as expected, the frequency of this firing increased as a function of applied current step. Although we observed a developmental increase in the amplitude of the fast AHP that normally regulates firing frequency, we found no corresponding developmental decline in firing frequency. On the contrary, we found additional evidence for a developmental increase in the excitability of Pf cells during PN 12–30. For example, the slope of the instantaneous firing frequency during the initial ISI, as well as the slope of the mean instantaneous firing frequency during the entire depolarizing pulse, both increased in parallel with the postnatal age of the animal regardless of cell type. The underlying ionic mechanism that is responsible for these changes remains to be determined, but is likely to involve an interplay between several voltage-dependent currents.

### Developmental changes in voltage-gated currents

We obtained evidence indicating that several different voltage-dependent currents are expressed by Pf cells, including the hyperpolarization-activated cation mediated Ih current, a transient potassium-mediated Ia-like current, the low-threshold calcium-mediated It current, and other rectifying membrane currents. The precise contribution of each of these currents to the excitability of Pf cells remains to be determined through selective pharmacological blockade. However, we did find evidence that Ih contributes to a postrebound excitation in Pf cells. Interestingly, the overall percentage of Ih-expressing Pf cells decreased with age, along with a corresponding decrease in the voltage-dependent slope of the amplitude of Ih. This indicates that the contribution of Ih to overall Pf cell excitability might decline with postnatal age (especially in Type I compared with Type II Ih expressing cells). Differential, age-dependent expression of Ih occurs during development in the CNS (Bender *et al.*, 2001). Furthermore, in some CNS neurons, there is an unequal distribution of Ih channels along the somatodendritic tree such that distal regions of the dendritic tree have higher densities of Ih compared with the soma and proximal dendrites (Berger *et al.*, 2001; Lorincz *et al.*, 2002). Such unequal distribution along the growing dendrites of Pf cells, given the long unramifying nature of the primary dendrites, potentially accounts for the developmental decline in the expression and amplitude of the Ih mediated ‘sag’ in membrane potential that we observed using sharp electrode intracellular current clamp recordings. Resolution of this issue awaits voltage-clamp recordings, especially from the dendrites of developing Pf cells.

The developmental change in Ih expression in Pf cells was not surprising given similar developmental changes in neuronal Ih expression elsewhere in the CNS. For example, we reported previously that there is a developmental increase and then decrease in the percentage of PPN cells expressing Ih over the same period (Kobayashi *et al.*, 2004a). The functional significance of these developmental changes in Ih-expression patterns is an area that deserves further attention, especially in light of the diverse roles of Ih channels in regulating the integrative and firing properties of neurons (Luthi *et al.*, 1998; Magee, 1998; Chen *et al.*, 2002; Robinson and Siegelbaum, 2003). In the PPN, for example, we found that there was a correlation between Ih expression and firing frequency such that those cells with Ih exhibited higher mean depolarization induced firing frequencies compared with non-Ih-expressing cells (Kobayashi *et al.*, 2004a). In the present study, we found essentially the opposite correlation, thus, cells with Ih had significantly lower mean firing frequencies. This is consistent with the reported role of dendritic Ih in dampening excitability. Although the overall excitability of Pf cells increased with age, the presence of Ih did not appear to alter this general developmental pattern. The mechanism by which Ih alters the firing frequency of Pf cells remains unknown. The interplay between Ih channels and other voltage-dependent channels offers a number of possibilities that must be explored. Particularly important from the aspect of thalamic function is the reported role of Ih in preferentially regulating synchronization of fast and slow activity (Migliore and Ferrante, 2004).

Although we identified a significant population of Pf cells with an apparent Ia current, there was no evidence of any significant developmental change in its expression with postnatal age. The presence of Ia contributes to a delay in the first AP evoked during a depolarizing current step as well as a delay in return to baseline after sufficient amplitude hyperpolarization (Huguenard *et al.*, 1991; McCormick and Huguenard, 1992). We found that an Ia-like current was expressed in both Pf cell types, but a higher percentage of Type I cells exhibited an Ia-like current compared with Type II cells. In the population of Pf cells as a whole, the delay to first AP during a depolarizing current step at threshold was nearly twice as long in Type I compared with Type II cells. This difference was most apparent when the cells were hyperpolarized to a holding potential of −80 mV, at which Ia-type currents are deinactivated enabling them to be activated to a greater degree during the subsequent membrane depolarizing test pulse (Huguenard *et al.*, 1991). The more noticeable presence of an Ia-like current in Type I compared with Type II cells might be important in the differential regulation of AP firing during brief depolarizations in the two cell types, as expected during fast excitatory synaptic responses.

Our analysis of the firing patterns of Pf cells included an investigation of developmental differences in the rebound response patterns. We identified three patterns: cells that did not exhibit rebound spiking (‘No Spike’ cells); cells that exhibited a rebound LTS-like response; and cells that exhibited a non-LTS rebound spiking response. There was a developmental change from ‘No Spike’ cells to ‘non-LTS spiking’ cells during the early portion of the period studied. Our data indicates that the non-LTS spiking response might be driven by residual Ih currents during the rebound depolarization. Similar contributions of Ih to rebound responses are described elsewhere in the CNS (Foehring and Waters, 1991; Rekling *et al.*, 1996; Koch and Grothe, 2003). The developmental shift in firing patterns that we observed might simply reflect maturation of conductances underlying AP generation, or an increase in Rin because we saw no corresponding increase in Ih expression. In contrast to the Ih-driven, non-LTS-induced rebound response, thalamic relay neurons typically exhibit a noticeable LTS component of the rebound response that drives slow rhythmic oscillations (Huguenard *et al.*, 1991; McCormick and Huguenard, 1992). It is reported that thalamic relay neurons have an adult-like expression of It by PN 14 and so are capable of repetitive oscillations early in postnatal development (Hernandez-Cruz and Pape, 1989; Perez Velazquez and Carlen, 1996; Warren and Jones, 1997; Tennigkeit *et al.*, 1998). In the intralaminar Pf nucleus, however, we found that the It current that underlies the LTS response was present in a minority of cells, regardless of postnatal age. Furthermore, the amplitude of these LTS responses was usually lower than that in neighboring thalamic relay nuclei. In most cells, the LTS only evoked a few APs, whereas in some cells it failed to evoke any APs. Similar failures have been noted in early developing thalamic neurons and even in some adult neurons (Warren and Jones, 1997). The lower amplitude of the LTS in Pf cells likely underlies the reduced number of APs given the known relationship between LTS amplitude and AP number in thalamic neurons (Zhan *et al.*, 2000). It is not known if there is a difference in the density, conductance or isoforms of It channels in Pf cells compared with other thalamic relay neurons.

The reduced amplitude of the LTS might also reflect the long unramifying nature of the proximal dendritic tree of Pf cells. If, for example, It channels in Pf cells are distributed primarily distally within the region of terminal dendritic branching, then the amplitude of such conductances would necessarily appear lower in amplitude in our somatic recordings. By contrast, a similar distribution in thalamic relay neurons might result in a higher conductance measured at the soma because of the more compact nature of the bushy dendritic trees of these neurons. Future experiments to define the distribution of voltage-gated channels along the somatodendritic trees of Pf cells will help resolve this issue. The degree to which Pf cells express Ia might also be important in this regard because dendritic Ia reduces It (Pape *et al.*, 1994). Pharmacological studies using specific channel blockers are needed to explore this possibility.

# DISCUSSION

## Lack of bipotential firing in Pf cells

In the classic description of the properties of thalamic neurons, nearly all of the 650 cells recorded in guinea pig thalamus (21 of which were in Pf or neighboring parts of the caudal thalamus) exhibited a similar 'bipotential firing pattern' characterized by the presence of prominent low-threshold calcium spike (LTS)-mediated burst firing (Jahnsen and Llinas, 1984a; Jahnsen and Llinas, 1984b; Jahnsen and Llinas, 1984c). That is, the cells fired in a tonic mode at depolarized levels and a burst mode at hyperpolarized membrane potentials. However, two of the 650 cells reported in that study lacked this distinct firing pattern, had no LTS and exhibited AP accommodation. These two cells were located in the posterior thalamus and in the lateral nucleus. The majority of Pf cells in our study exhibited firing properties similar to these two 'atypical' thalamic neurons in that they lacked prominent bipotential firing patterns. Even in the minority of Pf cells that did have an LTS-like response, the amplitude of this response was lower than in neighboring regions of the thalamus and only supported the generation of few APs. Changes in the holding potential of Pf cells did little to alter the overall firing pattern of the cells. Not surprisingly, therefore, none of our Pf cells displayed repetitive slow oscillations and they lacked the prominent plateau potentials that characterize classic thalamic relay neurons (Jahnsen and Llinas, 1984a; Jahnsen and Llinas, 1984b; Jahnsen and Llinas, 1984c). This indicates that cells in Pf have different firing properties than cells in neighboring regions of the intralaminar thalamus that do express rhythmic high frequency bursting behaviors (Steriade *et al.*, 1993).

This finding, coupled with the apparent maturational delay in Pf intrinsic membrane and AP properties, raises significant questions as to the exact role that the Pf plays in the development of overall thalamic function given that synchronous thalamic oscillations appear to develop soon after the second week postnatally (Mares *et al.*, 1982). There are several potential reasons that should be considered when trying to explain these differences in oscillatory potential of Pf cells compared with thalamocortical relay cells. First, we used a parasagittal slice preparation rather than transversely cut slices typically used in most studies. It is important to note that the somatodendritic morphology of the biocytin labeled Pf cells appeared relatively intact in our parasagittal slices. This indicates that the unique electrophysiological properties reported here do not reflect an artifact due to significant loss of dendritic arbors as a consequence of the parasagittal plane of sectioning. Second, although unlikely, we cannot rule out the possibility that the unique firing properties of Pf cells in this study reflected a loss of some intrinsic circuitry that is absent in our parasagittal slice preparation. For example, the reticular thalamus-Pf reciprocal circuitry is not likely to be retained in our slice preparation (especially in the parasagittal oblique oriented slices). It has been reported that reticular thalamic lesions *in vivo* result in significant decreases in Pf firing properties measured using extracellular recording techniques (Pollin *et al.*, 1997). Moreover, spindle oscillations are abolished in thalamic neurons disconnected from the reticular thalamus (Steriade *et al.*, 1985). Although the intracellular correlates of these changes in firing rates are unknown, it could underlie some of the differences we observed in this study, particularly with respect to the absence of repetitive oscillations. Third, our study concentrated on characterizing the postnatal development of Pf cells after thalamic relay neurons were mature. Unlike other thalamic nuclei cells that have been reported to be relatively mature by PN 14, we found that the postnatal development of Pf cells lagged behind (especially in Type II cells). The AP firing properties of Pf cells were still maturing up to the end of the first postnatal month, coinciding with the end of REM sleep development. However, it is unlikely that significant changes occurred after that time period since even those Pf cells that we recorded up to age PN 50 displayed the same type of general pattern of electrophysiological properties as cells at PN 30. Finally, it could simply be that the caudal region of medial Pf sampled in the present study

represents a functionally unique part of the intralaminar thalamus that possesses cells with distinct electrophysiological properties compared with other thalamocortical relay neurons. Interestingly, some of the properties of Pf cells are remarkably similar to those of thalamic interneurons including prominent AP accommodation, reduced It and slow ADPs (Pape and McCormick, 1995; Williams *et al.*, 1996; Zhu *et al.*, 1999). A difference in the electrophysiological properties of intralaminar Pf cells would not be unusual compared with thalamic relay neurons because higher-order thalamic neurons in the rat exhibit distinct properties compared with first order relay cells (Li *et al.*, 2003).

## Functional significance

The most intriguing finding of this study is that cells in the Pf represent a unique set of intralaminar neurons that differ dramatically from thalamic relay cells. Thus, the long recognized difference between the somatodendritic morphology of Pf and thalamic relay neurons might also extend to differences in their electrophysiological properties. One of the most prominent differences is the absence of rhythmic oscillatory firing in the Pf cells recorded in this study. This might be a reflection of the reduced or absent It current in Pf versus thalamic relay neurons. In addition, we found a reduced expression and apparent developmental decline in the manifestation of Ih in the same cells. The interplay between these two conductances underlies slow oscillations in thalamic relay neurons (Llinas, 1980; Huguenard and McCormick, 1992; McCormick and Huguenard, 1992). It is tempting to speculate that perhaps the contribution of It and Ih conductances to Pf cell physiology may change in certain disease states. Several studies have reported changes in the firing properties of Pf cells after deafferentation, such as the loss of intrathalamic and ascending sensory projections (Rinaldi *et al.*, 1991; Pollin *et al.*, 1997; Vaculin *et al.*, 2000). It would be interesting if there were increases in both the expression and/or efficacy of It and Ih channels in Pf cells after deafferentation, or in certain disease pathologies or aberrant developmental paradigms, such that a switch occurs in the electrophysiological properties of these cells results in the expression of a more classic oscillatory thalamic neuron physiology. Interestingly, it has been reported that cells in Pf exhibited a bursting pattern after lesions of the thalamic reticular nucleus, while control cells did not exhibit the same pattern (Pollin *et al.*, 1997). Unfortunately, the intracellular correlates of such changes in firing pattern have not been investigated. It is possible that the contributions of It and Ih channels to Pf cellular physiology may be altered in response to developmental or state-dependent differences in afferent inputs since both channels are regulated by various neurotransmitters. Of particular importance in this regard will be the effects of the cholinergic inputs to the Pf from the PPN nucleus.

The caudal intralaminar thalamic nuclei, including Pf and CL, represent the main thalamic target of the brainstem PPN nucleus (Steriade and Genn, 1982; Sugimoto and Hattori, 1984; Sofroniew *et al.*, 1985; Scarnati *et al.*, 1987; Hallanger and Wainer, 1988; Grunwerg *et al.*, 1992; Erro *et al.*, 1999; Oakman *et al.*, 1999; Capozzo *et al.*, 2003). These two nuclei, in turn, project to the cerebral cortex and basal ganglia structures (Steriade and Glenn, 1982; Jones, 1985; Sadikot *et al.*, 1990; Bentivolgio *et al.*, 1991; Sadikot *et al.*, 1992; Otake and Nakamura, 1998; Rudkin and Sadikot, 1999; Erro *et al.*, 1999; Lai *et al.*, 2000; Jones, 2002; van der Werf *et al.*, 2002). As such, ascending PPN inputs to these regions are likely to play an important role in regulating the sleep/wake cycle and in coordinating motor activity. In this regard, we have previously demonstrated that stimulation of the PPN elicits a prolonged response in cells in both of these regions (Kobayashi *et al.*, 2004a). However, differences in the frequency dependence of firing induced by different trains of PPN stimuli (10 vs 60 vs 90 Hz) in these two nuclei indicate that they differ in the manner in which they relay PPN information to the cortex and basal ganglia (Kobayashi *et al.*, 2004a).

This study represents a comprehensive study of the changes in electrophysiological properties of cells in the rat Pf intralaminar thalamic nucleus from the age at which thalamic relay neurons appear to reach maturity to the period during and after the developmental decrease in REM sleep. It has been suggested that REM sleep has the biological function of serving to direct the course of brain maturation (Marks *et al.*, 1995). This is in keeping with evidence that indicates that activity-dependent development might be a widespread mechanism that directs neural connectivity throughout the brain (Llinas, 1984; Marks *et al.*, 1995). Under this hypothesis, REM sleep could provide endogenous stimulation at a time when the brain has little or no exogenous input. Brainstem activation could contribute to the maturation of thalamocortical pathways. Therefore, the characteristics of electro-physiological properties of Pf neurons during this time are important to the understanding of REM sleep development.

In the rat, the critical period during early postnatal development in which the duration of REM sleep decreases corresponds to the PN 10–30 period (Jouvet-Mounier *et al.*, 1970). We have previously demonstrated that PPN neurons undergo dramatic differences in responsiveness to various neurotransmitters such as kainate, NMDA and serotonin, as well as intrinsic membrane properties during this time (Kobayashi *et al.*, 2003; Kobayashi *et al.*, 2004a; Kobayashi *et al.*, 2004b). The results of the present study indicate that neurons in the intralaminar Pf also undergo significant changes in excitability and AP properties during the same critical period. Just how the PPN–Pf pathway participates in the regulation of waking and REM sleep remains to be determined. It will be interesting to determine, for example, if the PPN projects to different populations of Pf cells. All Pf neurons in the rat represent projection neurons (Benson *et al.*, 1992), but there is a distinct topographical organization of the projection of medial versus lateral Pf cells (Feger *et al.*, 1994; Vercelli *et al.*, 2003; Yasukawa *et al.*, 2004). However, we do not know if the activity of Type I and Type II cells affect different forebrain targets. The apparent earlier maturation of Type I cells may indicate that they subserve some earlier maturing function, while Type II cells may play a larger role in later maturing events. It will be important to know how these properties change in various disease processes and perhaps contribute to the dysregulation of the sleep/wake cycle (Llinas *et al.*, 1999; Llinas *et al.*, 2001; Llinas and Ribary, 2001).

Thalamocortical dysrhythmia (TCD) appears to be the source for a number of neurological and psychiatric conditions, including neurogenic pain, tinnitus depression and Parkinson's Disease (Llinas *et al.*, 2001). The primary factor for the generation of TCD may be prolonged hyperpolarization due to disfacilitation (Curro Dossi *et al.*, 1992) or over-inhibition of thalamic neurons (Jeanmonod *et al.*, 2001). This state is characterized by the production of excessive LTS bursting in humans, not in anterodorsal or ventroposterior thalamus (Radhakrishnan *et al.*, 1999), but rather in the posterior Pf and CM (Jeanmonod *et al.*, 2001). This region, as described above, appears to be equivalent to the medial and lateral Pf in the rat (Jones, 1985), the same region sampled in the present studies. This is precisely the region to which small stereotaxic lesions are directed in order to alleviate the symptoms of these disorders (Jeanmonod *et al.*, 2001). Our results indicate that, for TCD to occur, the firing properties of Pf neurons must undergo marked changes, given the paucity of LTS-like bursting observed in intact animals. Further studies will be required to identify the potential mechanisms underlying such changes under pathological conditions, studies which will depend greatly on the descriptions of intact Pf neurons reported herein.

## Acknowledgements

This research was supported by USPHS grants NS20246 (EGR) and HD42199 (KDP). The authors thank Dr. Fang Zheng (Department of Pharmacology and Toxicology at UAMS) for valuable discussions during the preparation of the manuscript.

## References


Andersen E, Dafny N. An ascending serotonergic pain modulation pathway from the dorsal raphe nucleus to the parafascicularis nucleus of the thalamus. Brain Research 1983;269:57–67. [PubMed: 6871702]

Andrade R, Nicoll RA. Pharmacologically distinct actions of serotonin on single pyramidal neurones of the rat hippocampus recorded in vitro. Journal of Physiology 1987;394:99–124. [PubMed: 3443977]

Anna VM, Gemma GB, Laura AV, Pilar ST, Margarita MN. Intracranial self-stimulation in the parafascicular nucleus of the rat. Brain Research Bulletin 1999;48:401–406. [PubMed: 10357072]

Arai R, Jacobowitz DM, Deura S. Distribution of calretinin, calbindin-D28 k, and parvalbumin in the rat thalamus. Brain Research Bulletin 1994;33:595–614. [PubMed: 8187003]

Avanzini G, de Curtis M, Panzica F, Spreafico R. Intrinsic properties of nucleus reticularis thalami neurones of the rat studied in vitro. Journal of Physiology 1989;416:111–122. [PubMed: 2558172]

Bartlett EL, Smith PH. Anatomic, intrinsic, and synaptic properties of dorsal and ventral division neurons in rat medial geniculate body. Journal of Neurophysiology 1999;81:1999–2016. [PubMed: 10322042]

Bender RA, Brewster A, Santoro B, Ludwig A, Hofmann F, Biel M, et al. Differential and age-dependent expression of hyperpolarization-activated, cyclic nucleotide-gated cation channel isoforms 1–4 suggests evolving roles in the developing rat hippocampus. Neuroscience 2001;106:689–698. [PubMed: 11682156]

Benson DL, Isackson PJ, Gall CM, Jones EG. Contrasting patterns in the localization of glutamic acid decarboxylase and Ca2 +/calmodulin protein kinase gene expression in the rat central nervous system. Neuroscience 1992;46:825–849. [PubMed: 1311814]

Bentivoglio M, Balercia G, Kruger L. The specificity of the nonspecific thalamus: The midline nuclei. Brain Research 1991;87:53–80. [PubMed: 1678192]

Berger T, Larkum ME, Luscher HR. High I(h) channel density in the distal apical dendrite of layer V pyramidal cells increases bidirectional attenuation of EPSPs. Journal of Neurophysiology 2001;85:855–868. [PubMed: 11160518]

Capozzo A, Florio T, Cellini R, Moriconi U, Scarnati E. The pedunculopontine nucleus projection to the parafascicular nucleus of the thalamus: an electrophysiological investigation in the rat. Journal of Neural Transmission 2003;110:733–747. [PubMed: 12811634]

Celio MR. Calbindin D-28 k and parvalbumin in the rat nervous system. Neuroscience 1990;35:375–475. [PubMed: 2199841]

Chen K, Aradi I, Santhakumar V, Soltesz I. H-channels in epilepsy: new targets for seizure control? Trends in Pharmacological Sciences 2002;23:552–557. [PubMed: 12457772]

Curro Dossi R, Nunez A, Steriade M. Electrophysiology of a slow (0.5–4 Hz) intrinsic oscillation of cat thalamocortical neurons in vivo. Journal of Neurophysiology 1992;447:215–234.

Davies CH, Clarke VR, Jane DE, Collingridge GL. Pharmacology of postsynaptic metabotropic glutamate receptors in rat hippocampal CA1 pyramidal neurones. British Journal of Pharmacology 1995;116:1859–1869. [PubMed: 8528571]

Deschenes M, Bourassa J, Doan VD, Parent A. A single-cell study of the axonal projections arising from the posterior intralaminar thalamic nuclei in the rat. European Journal of Neuroscience 1996;8:329–343. [PubMed: 8714704]

Deschenes M, Bourassa J, Parent A. Two different types of thalamic fibers innervate the rat striatum. Brain Research 1995;701:288–292. [PubMed: 8925293]

Destexhe A, Babloyantz A, Sejnowski TJ. Ionic mechanisms for intrinsic slow oscillations in thalamic relay neurons. Biophysics Journal 1993a;65:1538–1552.

Destexhe A, Babloyantz A. A model of the inward current Ih and its possible role in thalamocortical oscillations. Neuroreport 1993;4:223–226. [PubMed: 8453063]

Destexhe A, Contreras D, Steriade M. Mechanisms underlying the synchronizing action of corticothalamic feedback through inhibition of thalamic relay cells. Journal of Neurophysiology 1998;79:999–1016. [PubMed: 9463458]

Destexhe A, McCormick DA, Sejnowski TJ. A model for 8–10 Hz spindling in interconnected thalamic relay and reticularis neurons. Biophysics Journal 1993b;65:2473–2477.

Erro E, Lanciego JL, Gimenez-Amaya JM. Relationships between thalamostriatal neurons and pedunculopontine projections to the thalamus: a neuroanatomical tract-tracing study in the rat. Experimental Brain Research 1999;127:162–170.

Feger J, Bevan M, Crossman AR. The projections from the parafascicular thalamic nucleus to the subthalamic nucleus and the striatum arise from separate neuronal populations: a comparison with the corticostriatal and corticosubthalamic efferents in a retrograde fluorescent double-labelling study. Neuroscience 1994;60:125–132. [PubMed: 8052406]

Fenelon G, Yelnik J, Francois C, Percheron G. Central complex of the primate thalamus:a quantitative analysis of neuronal morphology. Journal of Comparative Neurology 1994;342:463–479. [PubMed: 8021346]

Foehring RC, Waters RS. Contributions of low-threshold calcium current and anomalous rectifier (Ih) to slow depolarizations underlying burst firing in human neocortical neurons in vitro. Neuroscience Letters 1991;124:17–21. [PubMed: 1907002]

Frassoni C, Spreafico R, Bentivoglio M. Glutamate, aspartate and co-localization with calbindin in the medial thalamus an immunohistochemical study in the rat. Experimental Brain Research 1997;115:95–104.

Goaillard JM, Vincent P. Serotonin suppresses the slow after-hyperpolarization in rat intralaminar and midline thalamic neurones by activating 5-HT(7) receptors. Journal of Physiology 2002;541:453–465. [PubMed: 12042351]

Grunwerg BS, Krein H, Krauthamer GM. Somatosensory input and thalamic projection of pedunculopontine tegmental neurons. Neuroreport 1992;3:673–675. [PubMed: 1520853]

Guillazo-Blanch G, Vale-Martinez AM, Marti-Nicolovius M, Morgado-Bernal M, Cool-Andreu I. The parafascicular nucleus and two-way active avoidance: effects of electrical stimulation and electrode implantation. Experimental Brain Research 1999;129:605–614.

Hallanger AE, Wainer BH. Ascending projections from the pedunculopontine tegmental nucleus and the adjacent mesopontine tegmentum in the rat. Journal of Comparative Neurology 1988;274:483–515. [PubMed: 2464621]

Harris RM. Morphology of physiologically identified thalamo-cortical relay neurons in the rat ventrobasal thalamus. Journal of Comparative Neurology 1986;251:491–505. [PubMed: 2431010]

Harte SE, Lagman AL, Borszcz GS. Antinociceptive effects of morphine injected into the nucleus parafascicularis thalami of the rat. Brain Research 2000;874:78–86. [PubMed: 10936226]

Hazlett JC, Dutta CR, Fox CA. The neurons in the centromedian-parafascicular complex of the monkey (Macaca mulatta): a Golgi study. Journal of Comparative Neurology 1976;168:41–73. [PubMed: 819469]

Hazlett JC, Hazlett LD. Long axon neurons in the parafascicular and parafascicular posterolateral nuclei of the opossum: a Golgi study. Brain Research 1977;136:543–546. [PubMed: 72588]

Henderson JM, Carpenter K, Cartwright H, Halliday GM. Degeneration of the centre-median-parafascicular complex in parkinson's disease. Annals of Neurology 2000;47:345–352. [PubMed: 10716254]

Hermenegildo SH, Anna VM, Gemma GB, Margarita MN, Roser NA, Ignacio MB. Differential effects of parafascicular electrical stimulation on active avoidance depending on the retention time, in rats. Brain Research Bulletin 2000;52:419–426. [PubMed: 10922522]

Hernandez-Cruz A, Pape HC. Identification of two calcium currents in acutely dissociated neurons from the rat lateral geniculate nucleus. Journal of Neurophysiology 1989;61:1270–1283. [PubMed: 2501459]

Huguenard JR, Coulter DA, Prince DA. A fast transient potassium current in thalamic relay neurons:kinetics of activation and inactivation. Journal of Neurophysiology 1991;66:1304–1315. [PubMed: 1662262]

Huguenard JR, McCormick DA. Simulation of the currents involved in rhythmic oscillations in thalamic relay neurons. Journal of Neurophysiology 1992;68:1373–1383. [PubMed: 1279135]

Jahnsen H, Llinas R. Ionic basis for the electro-responsiveness and oscillatory properties of guinea-pig thalamic neurones in vitro. Journal of Physiology 1984a;349:227–247. [PubMed: 6737293]

Jahnsen H, Llinas R. Electrophysiological properties of guinea-pig thalamic neurones: an in vitro study. Journal of Physiology 1984b;349:205–226. [PubMed: 6737292]

Jahnsen H, Llinas R. Voltage-dependent burst-to-tonic switching of thalamic cell activity: an in vitro study. Archives Italiens de Biologie 1984c;122:73–82.

Jeanmonod D, Magnin M, Morel A, Siegemund M, Cancro A, Lanz M, et al. Thalamocortical dysrhythmia II. Clinical and surgical aspects. Thalamus & Related Systems 2001;1:245–254.

Jones EG. Thalamic organization and function after Cajal. Brain Research 2002;136:333–357. [PubMed: 12143393]

Jones, EG. The Thalamus. Plenum Press; New York: 1985.

Jouvet-Mounier D, Astic L, Lacote D. Ontogenesis of the states of sleep in rat, cat, and guinea pig during the first postnatal month. Developmental Psychobiology 1970;2:216–239. [PubMed: 5527153]

Kawaguchi Y. Physiological, morphological, and histochemical characterization of three classes of interneurons in rat neostriatum. Journal of Neuroscience 1993;13:4908–4923. [PubMed: 7693897]

Kobayashi T, Good C, Biedermann J, Barnes C, Skinner RD, Garcia-Rill E. Developmental changes in pedunculopontine nucleus (PPN) neurons. Journal of Neurophysiology 2004a;91:1470–1481. [PubMed: 15010495]

Kobayashi T, Good C, Mamiya K, Skinner RD, Garcia-Rill E. Development of REM sleep drive and clinical implications. Journal of Applied Physiology 2004b;96:735–746. [PubMed: 14527968]

Kobayashi T, Homma Y, Good C, Skinner RD, Garcia-Rill E. Developmental changes in the effects of serotonin on neurons in the region of the pedunculopontine nucleus. Developmental Brain Research 2003;140:57–66. [PubMed: 12524176]

Koch U, Grothe B. Hyperpolarization-activated current (Ih) in the inferior colliculus: distribution and contribution to temporal processing. Journal of Neurophysiology 2003;90:3679–3687. [PubMed: 12968010]

Lai H, Tsumori T, Shiroyama T, Yokota S, Nakano K, Yasui Y. Morphological evidence for a vestibulo-thalamo-striatal pathway via the parafascicular nucleus in the rat. Brain Research 2000;872:208–214. [PubMed: 10924695]

Li J, Bickford ME, Guido W. Distinct firing properties of higher order thalamic relay neurons. Journal of Neurophysiology 2003;90:291–299. [PubMed: 12634282]

Liu FY, Qiao JT, Dafny N. Cerebellar stimulation modulates thalamic noxious-evoked responses. Brain Research Bulletin 1993;30:529–534. [PubMed: 8457903]

Llinas R, Ribary U. Consciousness and the Brain. The thalamocortical dialogue in health and disease. Annals of the New York Academy of Sciences 2001;929:166–175. [PubMed: 11349424]

Llinas R, Ribary U, Jeanmonod D, Cancro R, Kronberg E, Schulman J, et al. Thalamocortical dysrhythmia I. Functional and imaging aspects. Thalamus & Related Systems 2001;1:237–244.

Llinas R, Ribary U, Jeanmonod D, Kronberg E, Mitra PP. Thalamocortical dysrhythmia: a neurological and neuropsychiatric syndrome characterized by magnetoencephalography. Proceedings of the National Academy of Sciences 1999;96:15222–15227.

Llinas RR. The intrinsic electrophysiological properties of mammalian neurons: insights into central nervous system function. Science 1980;242:1654–1664. [PubMed: 3059497]

Llinas, RR. Possible role of tremor in the organization of the nervous system. In: Findley, LJ.; Capildeo, R., editors. International Neurological Symposium on Tremor. MacMillan Press; London, UK: 1984. p. 473-478.

Lorincz A, Notomi T, Tamas G, Shigemoto R, Nusser Z. Polarized and compartment-dependent distribution of HCN1 in pyramidal cell dendrites. Nature Neuroscience 2002;5:1185–1193.

Luthi A, Bal T, McCormick DA. Periodicity of thalamic spindle waves is abolished by ZD7288, a blocker of Ih. Journal of Neurophysiol 1998;79:3284–3289.

MacLeod N, Turner C, Edgar J. Properties of developing lateral geniculate neurones in the mouse. International Journal of Developmental Neuroscience 1997;15:205–224. [PubMed: 9178039]

Magee JC. Dendritic hyperpolarization-activated currents modify the integrative properties of hippocampal CA1 pyramidal neurons. Journal of Neuroscience 1998;18:7613–7624. [PubMed: 9742133]

Malenka RC, Madison DV, Andrade R, Nicoll RA. Phorbol esters mimic some cholinergic actions in hippocampal pyramidal neurons. Journal of Neuroscience 1986;6:475–480. [PubMed: 3456434]

Mares P, Maresova D, Trojan S, Fischer J. Ontogenetic development of rhythmic thalamo-cortical phenomena in the rat. Brain Research Bulletin 1982;8:765–769. [PubMed: 7139363]

Marks GA, Shaffery JP, Oksenberg A, Speciale SG, Roffwarg HP. A functional role for REM sleep in brain maturation. Behavioural Brain Research 1995;69:1–11. [PubMed: 7546299]

Matsumoto N, Minamimoto T, Graybiel AM, Kimura M. Neurons in the thalamic CM-Pf complex supply striatal neurons with information about behaviorally significant sensory events. Journal of Neurophysiology 2001;85:960–976. [PubMed: 11160526]

McCormick DA, Bal T. Sleep and arousal: thalamocortical mechanisms. Annual Review of Neuroscience 1997;20:185–215.

McCormick DA, Huguenard JR. A model of the electro-physiological properties of thalamocortical relay neurons. Journal of Neurophysiology 1992;8:1384–1400. [PubMed: 1331356]

McCormick DA, Pape HC, Williamson A. Actions of norepinephrine in the cerebral cortex and thalamus: implications for function of the central noradrenergic system. Progress in Brain Research 1991;88:293–305. [PubMed: 1726028]

Migliore M, Messineo L, Ferrante M. Dendritic Ih selectively blocks temporal summation of unsynchronized sistal inputs in CA1 pyramidal neurons. Journal of Computational Neuroscience 2004;16:5–13. [PubMed: 14707540]

Minamimoto T, Kimura M. Participation of the thalamic CM-Pf complex in attentional orienting. Journal of Neurophysiology 2002;87:3090–3101. [PubMed: 12037210]

Oakman SA, Faris PL, Cozzari C, Hartman BK. Characterization of the extent of pontomesencephalic cholinergic neurons projecting to the thalamus: comparison with projections to midbrain dopaminergic groups. Neuroscience 1999;94:529–547. [PubMed: 10579214]

Otake K, Nakamura T. Single midline thalamic neurons projecting to both the ventral striatum and the prefrontal cortex in the rat. Neuroscience 1998;86:635–649. [PubMed: 9881876]

Pape HC, Budde T, Mager R, Kisvarday ZF. Prevention of Ca(2+)-mediated action potentials in GABAergic local circuit neurones of rat thalamus by a transient K+ current. Journal of Physiology 1994;478:403–422. [PubMed: 7965855]

Pape HC, McCormick DA. Electrophysiological and pharmacological properties of interneurons in the cat dorsal lateral geniculate nucleus. Neuroscience 1995;68:1105–1125. [PubMed: 8544986]

Pare D, Smith Y, Parent A, Steriade M. Projections of brainstem core cholinergic and non-cholinergic neurons of cat to intralaminar and reticular thalamic nuclei. Neuroscience 1988;25:69–86. [PubMed: 3393287]

Parent M, Parent A. Single-axon tracing and three-dimensional reconstruction of centre median-parafascicular thalamic neurons in primates. Journal of Comparative Neurology 2005;48:127–144. [PubMed: 15558721]

Pearson JC, Norris JR, Phelps CH. The cytoarchitecture and some efferent projections of the centromedian-parafascicular complex in the lesser bushbaby (Galago senegalensis). Journal of Comparative Neurology 1984;225:554–569. [PubMed: 6203940]

Pedroarena C, Llinas R. Dendritic calcium conductances generate high-frequency oscillation in thalamocortical neurons. Proceedings of the National Academy of Sciences 1997;94:724–728.

Perez Velazquez JL, Carlen PL. Development of firing patterns and electrical properties in neurons of the rat ventrobasal thalamus. Developmental Brain Research 1996;91:164–170. [PubMed: 8852366]

Phelan KD, Deere T, Mahler HR, Garcia-Rill E. Intrinsic membrane properties of rat parafascicular thalamic nucleus neurons recorded in vitro. Neuroscience Abstracts 2002;28:32.1.

Pollin B, Joulin Y, Amsallem B, Rokyta R, Cesaro P. Abnormal neuronal activities in intralaminar thalamic nuclei following chronic lesions of nucleus reticularis thalami in rats. Physiology Research 1997;46:475–485.

Radhakrishnan V, Tsoukatos J, Davis KD, Tasker RR, Lozano AM, Dostrovsky JO. A comparison of the burst activity of lateral thalamic neurons in chronic pain and non-pain patients. Pain 1999;80:567–575. [PubMed: 10342418]

Rekling JC, Champagnat J, Denavit-Saubie M. Electroresponsive properties and membrane potential trajectories of three types of inspiratory neurons in the newborn mouse brain stem in vitro. Journal of Neurophysiology 1996;75:795–810. [PubMed: 8714653]

Resibois A, Rogers JH. Calretinin in rat brain:an immunohistochemical study. Neuroscience 1992;46:101–134. [PubMed: 1594096]

Rinaldi PC, Young RF, Albe-Fessard D, Chodakiewitz J. Spontaneous neuronal hyperactivity in the medial and intralaminar thalamic nuclei of patients with deafferentation pain. Journal of Neurosurgery 1991;74:415–421. [PubMed: 1993906]

Robinson RB, Siegelbaum SA. Hyperpolarization-activated cation currents: from molecules to physiological function. Annual Review of Physiology 2003;65:453–480.

Rub U, Del Tredici K, Del Turco D, Braak H. The intralaminar nuclei assigned to the medial pain system and other components of this system are early and progressively affected by the Alzheimer's disease-related cytoskeletal pathology. Journal of Chemical Neuroanatomy 2002;23:279–290. [PubMed: 12048111]

Rudkin TM, Sadikot AF. Thalamic input to parvalbumin-immunoreactive gabaergic interneurons: organization in normal striatum and effect of neonatal decortication. Neuroscience 1999;88:1165–1175. [PubMed: 10336127]

Sadikot AF, Parent A, Francois C. Efferent connections of the centromedian and parafascicular thalamic nuclei in the squirrel monkey: a PHA-L study of subcortical projections. Journal of Comparative Neurology 1992;315:137–159. [PubMed: 1372010]

Sadikot AF, Parent A, Francois C. The centre median and parafascicular thalamic nuclei project respectively to the sensorimotor and associative-limbic striatal territories in the squirrel monkey. Brain Research 1990;510:161–165. [PubMed: 1691043]

Sano K, Yoshioka M, Ogashiwa M, Ishijima B, Ohye C. Thalamolaminotomy. A new operation for relief of intractable pain. Confinia Neurologica 1966;27:63–66. [PubMed: 5955975]

Sawyer SF, Young SJ, Groves PM. Quantitative Golgi study of anatomically identified subdivisions of motor thalamus in the rat. Journal of Comparative Neurology 1989;286:1–27. [PubMed: 2475532]

Scarnati E, Gasbarri A, Campana E, Pacitti C. The organization of nucleus tegmenti pedunculopontinus neurons projecting to basal ganglia and thalamus: a retrograde fluorescent double labeling study in the rat. Neuroscience Letters 1987;79:11–16. [PubMed: 3670718]

Sofroniew MV, Priestley JV, Consolazione A, Eckenstein F, Cuello AC. Cholinergic projections from the midbrain and pons to the thalamus in the rat, identified by combined retrograde tracing and choline acetyltransferase immunohistochemistry. Brain Research 1985;329:213–223. [PubMed: 3978443]

Steriade M, Glenn LL. Neocortical and caudate projections of intralaminar thalamic neurons and their synaptic excitation from midbrain reticular core. Journal of Neurophysiology 1982;48:352–371. [PubMed: 6288887]

Steriade M, Deschenes M, Domich L, Mulle C. Abolition of spindle oscillations in thalamic neurons disconnected from nucleus reticularis thalami. Journal of Neurophysiology 1985;54:1473–1497. [PubMed: 4087044]

Steriade M, Curro Dossi R, Contreras D. Electrophysiological properties of intralaminar thalamocortical cells discharging rhythmic (approximately 40 HZ) spike-bursts at approximately 1000 HZ during waking and rapid eye movement sleep. Neuroscience 1993;56:1–9. [PubMed: 8232908]

Steriade, M. Cellular substrates of oscillations in corticothalamic systems during states of vigilance. In: Lydic, R.; Baghdoyan, HA., editors. Handbook of Behavioral State Control. Cellular and molecular mechanisms. CRC Press; New York: 1999. p. 327-347.

Sugimoto T, Hattori T. Organization and efferent projections of nucleus tegmenti pedunculopontinus pars compacta with special reference to its cholinergic aspects. Neuroscience 1984;11:931–946. [PubMed: 6738860]

Sugiyama K, Muteki T, Shimoji K. Halothane-induced hyperpolarization and depression of postsynaptic potentials of guinea pig thalamic neurons in vitro. Brain Research 1992a;576:97–103. [PubMed: 1515914]

Sugiyama K, Ryu H, Uemura K. Identification of nociceptive neurons in the medial thalamus: morphological studies of nociceptive neurons with intracellular injection of horseradish peroxidase. Brain Research 1992b;586:36–43. [PubMed: 1380880]

Tennigkeit F, Schwarz DW, Puil E. Postnatal development of signal generation in auditory thalamic neurons. DevelopmentalBrain Research 1998;109:255–263.

Uematsu S, Konigsmark B, Walker AE. Thalamotomy for alleviation of intractable pain. Confinia Neurologica 1974;36:88–96. [PubMed: 4132896]

Vaculin S, Franek M, Rokyta R. Dorsal rhizotomy changes the spontaneous neuronal activity of nuclei in the medial thalamus. Physiology Research 2000;49:279–283.

Vale-Martinez A, Guillazo-Blanch G, Aldavert-Vera L, Segura-Tores P, Marti-Nicolovius M. Intracranial self-stimulation in the parafascicular nucleus of the rat. Brain Research Bulletin 1999;48:401–406. [PubMed: 10357072]

Van der Werf YD, Witter MP, Groenewegen HJ. The intralaminar and midline nuclei of the thalamus. Anatomical and functional evidence for participation in processes of arousal and awareness. Brain Research Reviews 2002;39:107–140. [PubMed: 12423763]

Vasilyev DV, Barish ME. Postnatal development of the hyperpolarization-activated excitatory current ih in mouse hippocampal pyramidal neurons. Journal of Neuroscience 2002;22:8992–9004. [PubMed: 12388606]

Velasco M, Brito F, Jimenez F, Gallegos M, Velasco AL, Velasco F. Effect of fentanyl and naloxone on a thalamic induced painful response in intractable epileptic patients. Stereotactic and Functional Neurosurgery 1998;71:90–102. [PubMed: 10087473]

Vercelli A, Marini G, Tredici G. Anatomical organization of the telencephalic connections of the parafascicular nucleus in adult and developing rats. European Journal of Neuroscience 2003;18:275–289. [PubMed: 12887409]

Warren RA, Jones EG. Maturation of neuronal form and function in a mouse thalamo-cortical circuit. Journal of Neuroscience 1997;17:277–295. [PubMed: 8987755]

Whittle IR, Jenkinson JL. CT-guided stereotactic antero-medial pulvinotomy and centromedian-parafascicular thalamotomy for intractable malignant pain. British Journal of Neurosurgery 1995;9:195–200. [PubMed: 7632366]

Williams SR, Turner JP, Anderson CM, Crunelli V. Electrophysiological and morphological properties of interneurones in the rat dorsal lateral geniculate nucleus in vitro. Journal of Physiology 1996;490:129–147. [PubMed: 8745283]

Yasukawa T, Kita T, Xue Y, Kita H. Rat intralaminar thalamic nuclei projections to the globus pallidus: a biotinylated dextran amine anterograde tracing study. Journal of Comparative Neurology 2004;471:153–167. [PubMed: 14986309]

Young RF, Jacques DS, Rand RW, Copcutt BC, Vermeulen SS, Posewitz AE. Technique of stereotactic medial thalamotomy with the Leksell Gamma Knife for treatment of chronic pain. Neurology Research 1995a;17:59–65.

Young RF, Vermeulen SS, Grimm P, Posewitz AE, Jacques DB, Rand RW, et al. Gamma Knife thalamotomy for the treatment of persistent pain. Stereotactic and Functional Neurosurgery 1995b; 64:172–181. [PubMed: 8584825]

Zhan XJ, Cox CL, Sherman SM. Dendritic depolarization efficiently attenuates low-threshold calcium spikes in thalamic relay cells. Journal of Neuroscience 2000;20:3909–3914. [PubMed: 10804230]

Zhu JJ, Uhlrich DJ, Lytton WW. Burst firing in identified rat geniculate interneurons. Neuroscience 1999;91:1445–1460. [PubMed: 10391450]

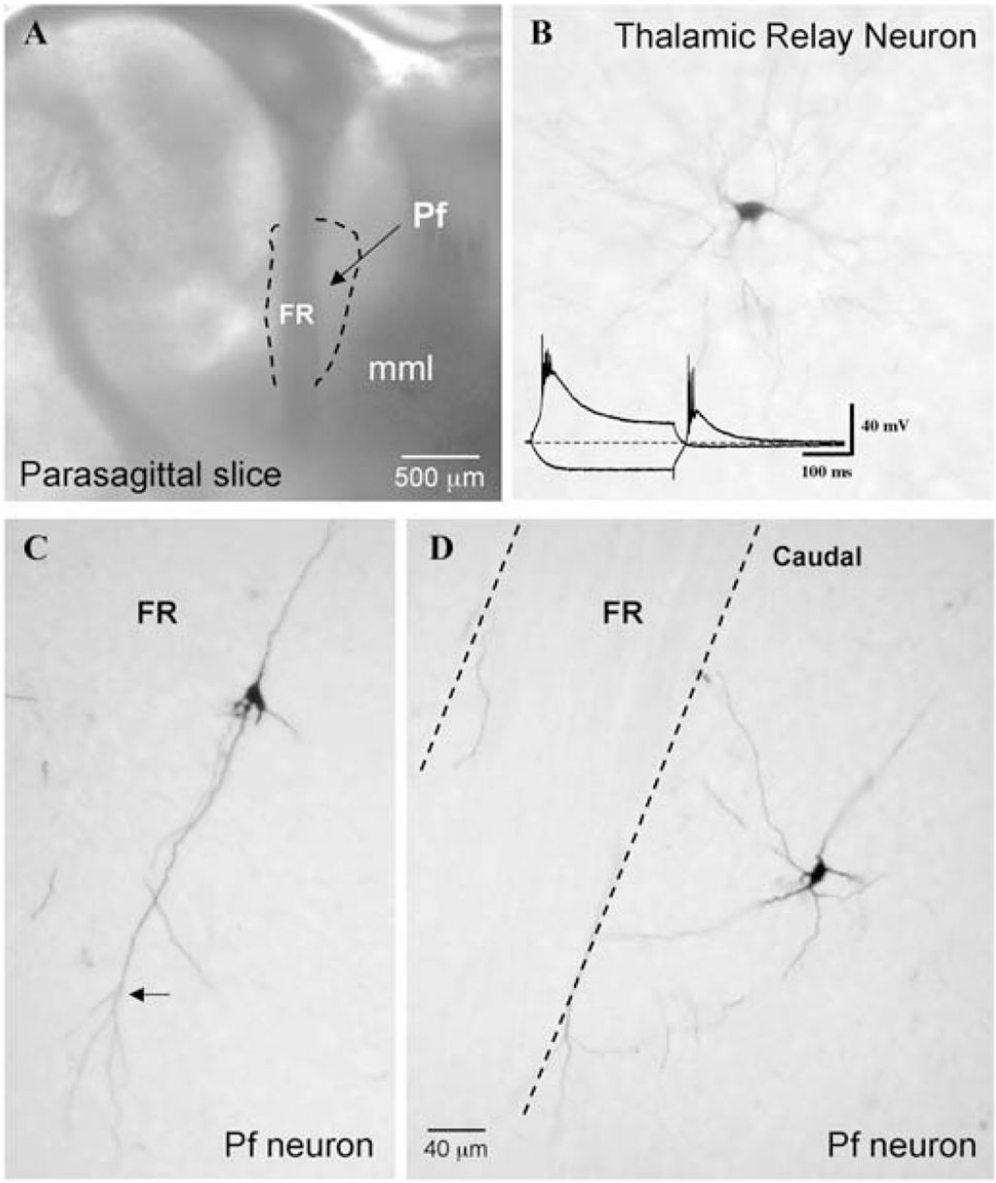


**Fig. 1. Recording location and Pf cell morphology**

(A) Photomicrograph of the parasagittal slice used to record Pf neurons, as viewed under a dissecting microscope. Recordings were restricted to within the confines of the dotted outline surrounding the fasciculus retroflexus (FR). (mml, medial medullary lamina). (B) Example of a biocytin labeled thalamic relay cell located rostral to Pf in the parasagittal slice. The inset shows the large amplitude LTS that characterize such cells. (C, D) Two biocytin-injected cells with the long unramified dendrites of Pf cells compared with the compact bushy dendritic trees typical of neighboring thalamic relay neurons (as in B). Calibration bars: A, 500 μm (inset: vertical 40 mV; horizontal 100 ms); B–D, 40 μm).

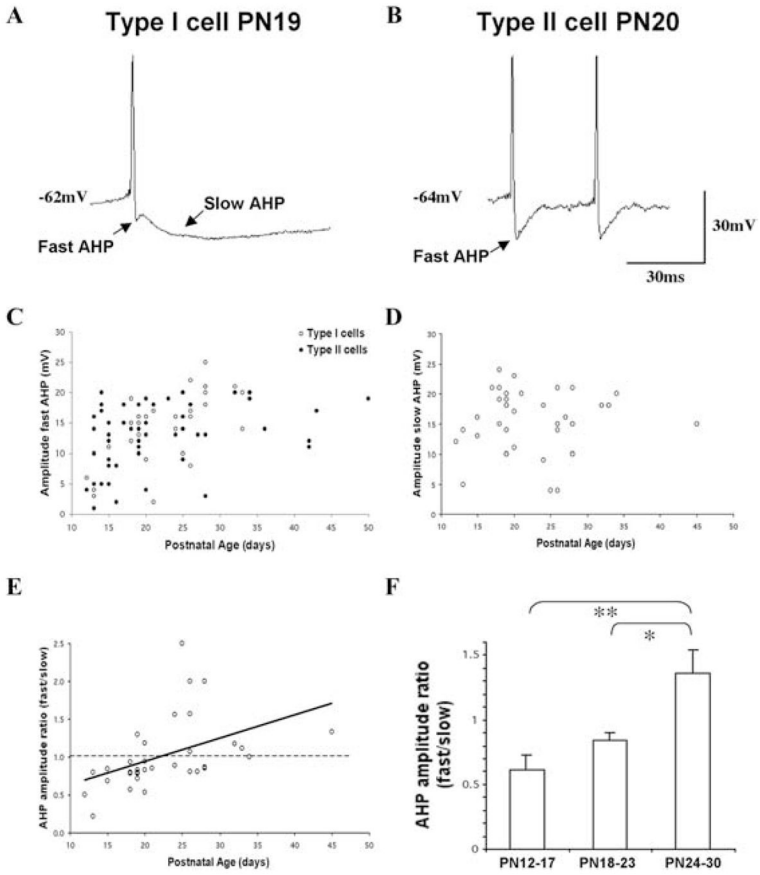


**Fig. 2. Two types of Pf cells**

(A, B) Shape of action potentials (APs) exhibited by representative Type I (A) and Type II (B) cells. Each cell type had a fast AP AHP, but only Type I cells exhibited a prominent slow AHP. Calibration bars: vertical 30 mV; horizontal 30 ms. (C) Fast AHP amplitude plotted as a function of age and cell type. Type I cells (open circles), Type II cells (filled circles) in this and subsequent figures. (D) Slow AHP amplitude of Type I cells plotted as a function of age. (E) Fast AHP:slow AHP amplitude in individual Type I cells plotted as a function of age. The solid line represents the regression line. (F) Comparison of the mean AHP amplitude ratio (fast AHP:slow AHP) in early postnatal Type I cells grouped into six postnatal day periods (mean ±S.E., $*P < 0.05$, $**P < 0.01$).

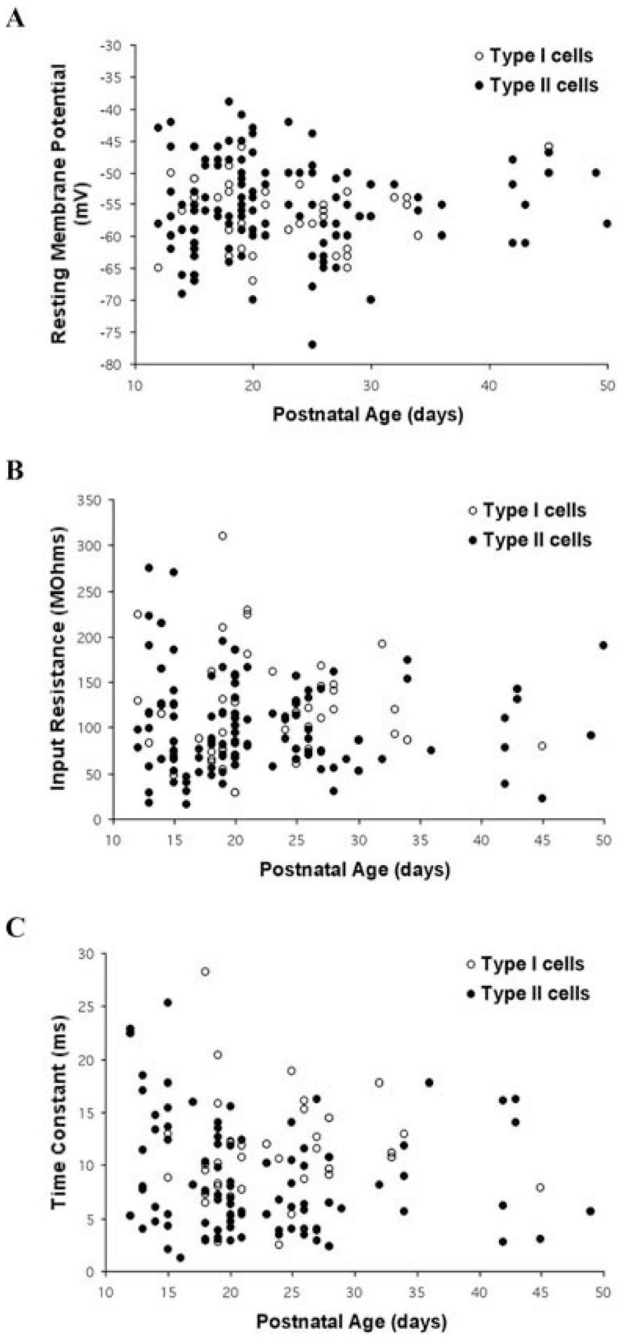


**Fig. 3. Developmental changes in the intrinsic membrane properties of Pf cells**

The (A) resting membrane potential (RMP), (B) input resistance (Rin), and (C) membrane time constant are plotted as a function of age and cell type. Note overlapping properties and consistency across development.

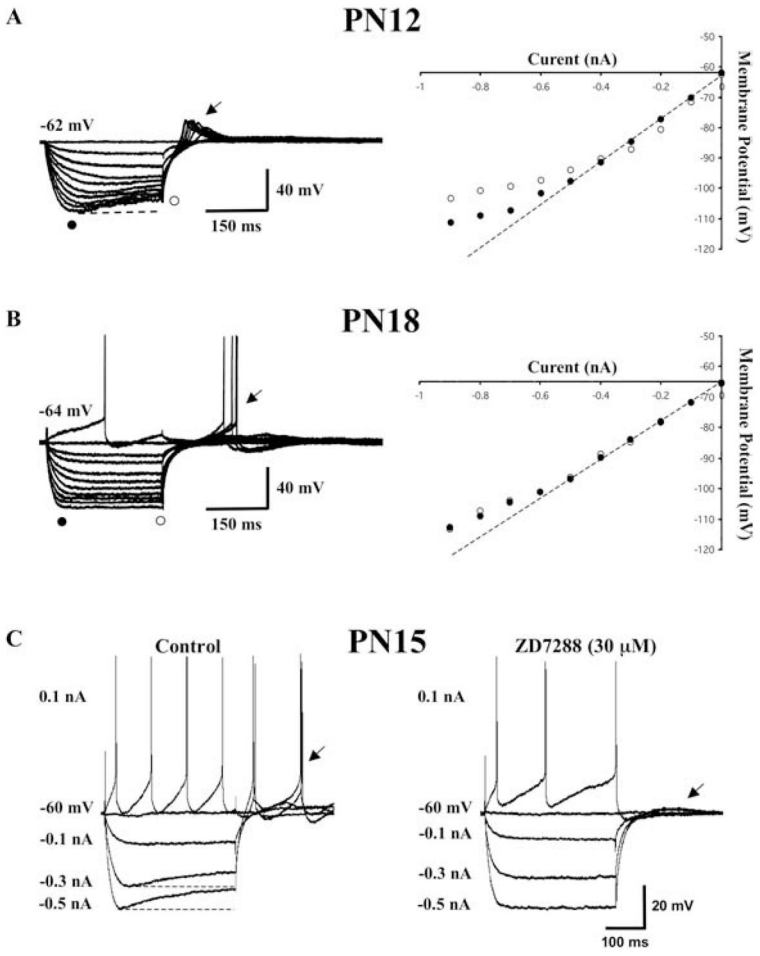


**Fig. 4. Non-linearity in the current-voltage (I–V) relationship of Pf cells**

(A) Representative current-clamp recordings from a PN 12 Pf neuron in response to a series of hyperpolarizing current pulses (0.1–0.9 nA). This cell exhibited a prominent hyperpolarization-activated (Ih) current reflected as a depolarizing 'sag' in the membrane potential (left side). The voltage-dependence of Ih is reflected by the difference between the peak (solid circle) and plateau (open circle), I–V plots for this cell are shown on the right. (B) Representative recordings from a PN 18 Pf cell that lacked an Ih current (left side). Note the absence of any difference in the peak and plateau, which is reflected in the I–V plot on the right side. The cells in A and B have a non-Ih inward membrane rectification reflected by the deviation of the peak (solid circle) in the I–V plots at hyperpolarized membrane potentials compared with the linear portion of the I–V plot shown by the dotted line. Calibration bars: vertical 40 mV; horizontal 150 ms. (C) The late developing inward rectifying Ih current in this PN 15 Pf cell (left side) was blocked by ZD-7288 (30 μM) (right side) indicating that it represented an Ih current. Note the absence of rebound depolarizing action potentials once the Ih current had been blocked (compare left vs right arrows). Calibration bars: vertical 20 mV; horizontal 100 ms.

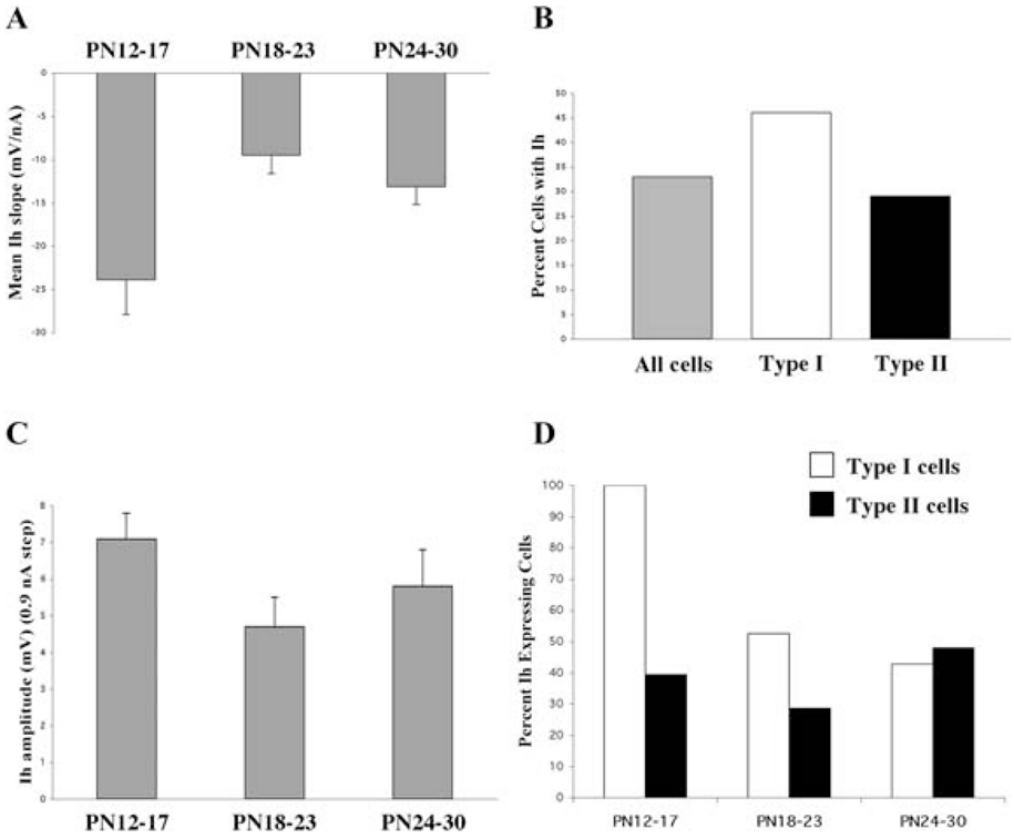


**Fig. 5. Developmental changes in hyperpolarization-activated (Ih) currents in Pf cells**

(A) Mean slope of the Ih voltage deflection plotted as a function of age group (mean ±S.E.). (B) Comparison of the percent of Ih-expressing cells in the total Pf population compared with the percentage in Type I and Type II cells. (C) Maximum Ih amplitude measured in response to a 0.9 nA current step plotted as a function of age group (mean ±S.E.). (D) Percent of Type I and Type II cells expressing Ih plotted as a function of age group.

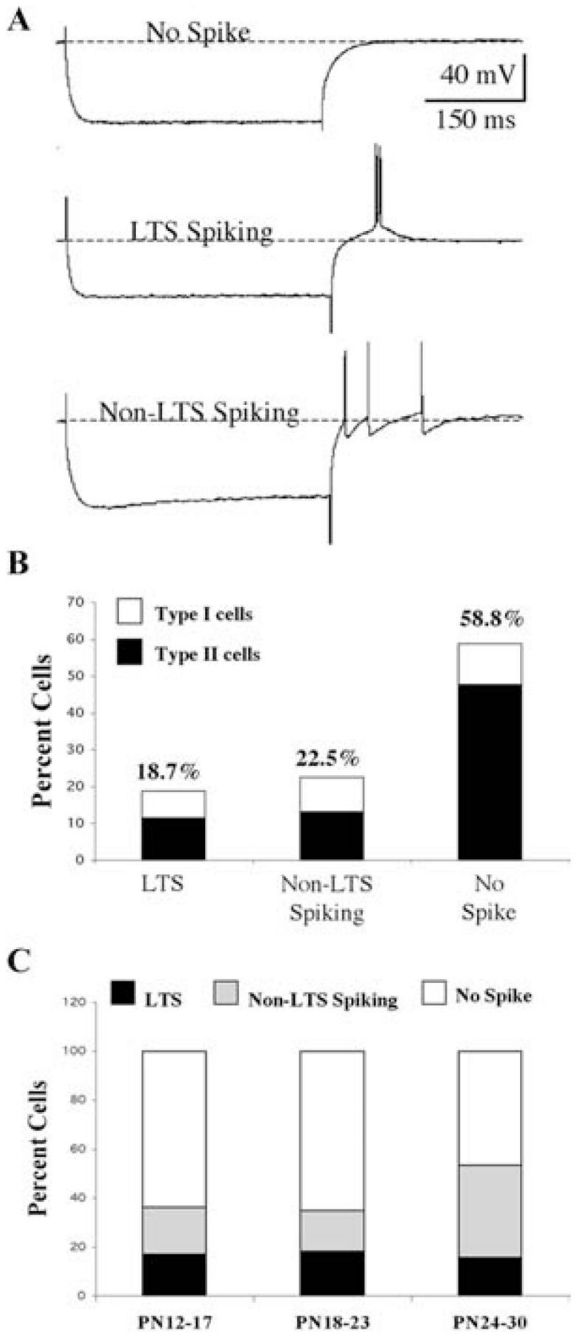


**Fig. 6. Developmental changes in the rebound firing patterns displayed by Pf cells**

(A) Examples of the three types of rebound responses seen in Pf cells: No spike (top); low-threshold spike (LTS)-like spiking (middle); and non-LTS spiking (bottom). (B) Distribution of Type I and Type II cells with respect to the rebound response pattern. (C) Developmental changes in rebound response pattern plotted as a function of age group. LTS (filled bars), non-LTS spiking (shaded bars) and no spike (open bars). Note developmental decrease in no spike cells.

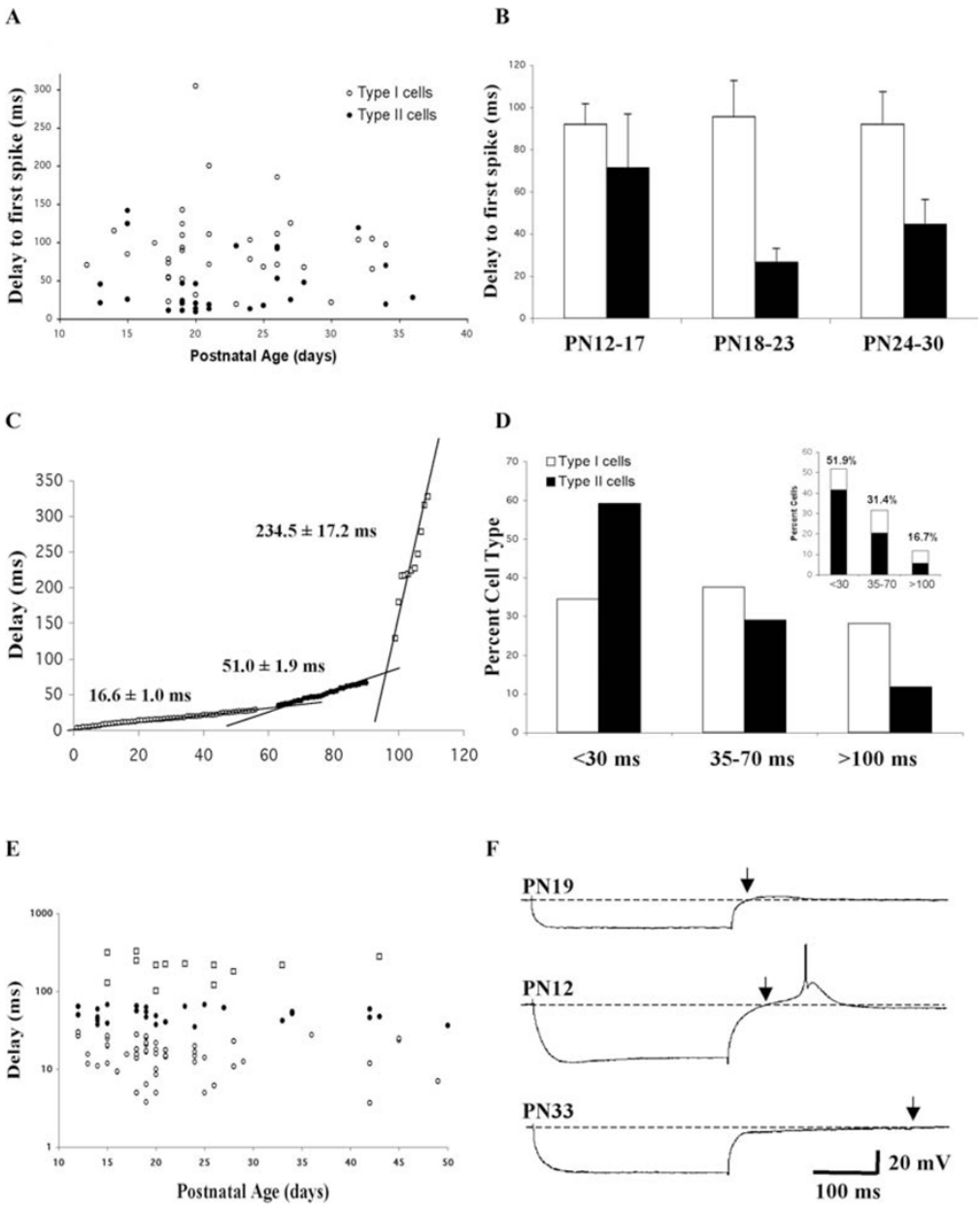


**Fig. 7. Transient potassium (Ia-like) current expression in developing Pf cells**

(A) Delay to first spike (Ia-like current effect) plotted as a function of postnatal age and cell type. The delay was measured in response to threshold depolarizing current steps from a holding potential of −60 mV. (B) Comparison of the mean delay to first spike in Type I and Type II cells plotted as a function of age group. (C) Sorted graph of the delay step to the return to baseline membrane potential following a 0.5 nA hyperpolarizing current step in cells held at −60 mV. Three groups [short delay, open circles; medium delay, filled circles; and long delay, open squares) could be discerned on the basis of population regression lines. See text for description of the three delay groups. Points at the intersections have been deleted for clarity. (D) Percent distribution of Type I and Type II cells plotted as a function of the three different return to baseline delay groups. Inset: The contribution of Type I and Type II cells to each delay group. (E) Distribution of cells in the three different return to baseline delay groups plotted as a function of age. (F) Representative examples of the three different return to baseline

delay patterns in Pf cells. Short delay, PN 19 cell, top recording; medium delay, PN 12 cell, middle recording; long delay, PN 33 cell, bottom recording. Arrows mark the point of return to baseline. Calibration bars: vertical 20 mV; horizontal 100 ms.

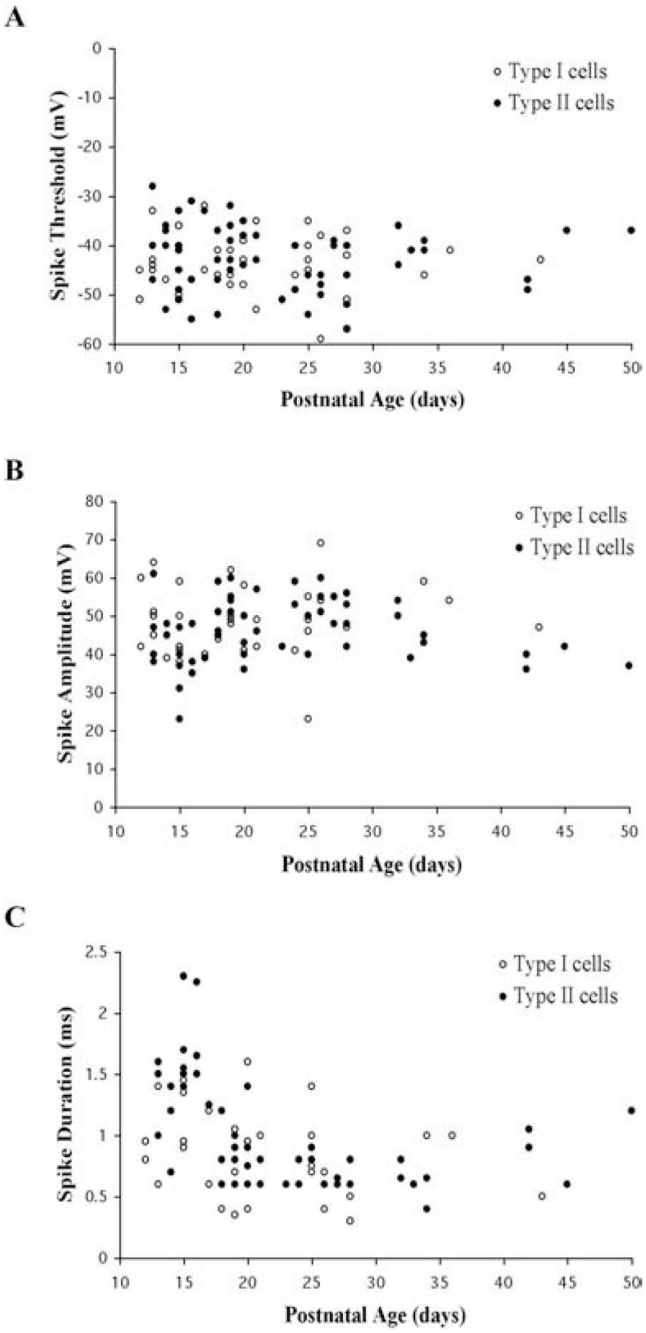


**Fig. 8. Developmental changes in the AP properties of Pf cells**

The (A) AP threshold, (B) AP amplitude, and (C) half-amplitude AP duration are plotted as a function of age and Pf cell type.

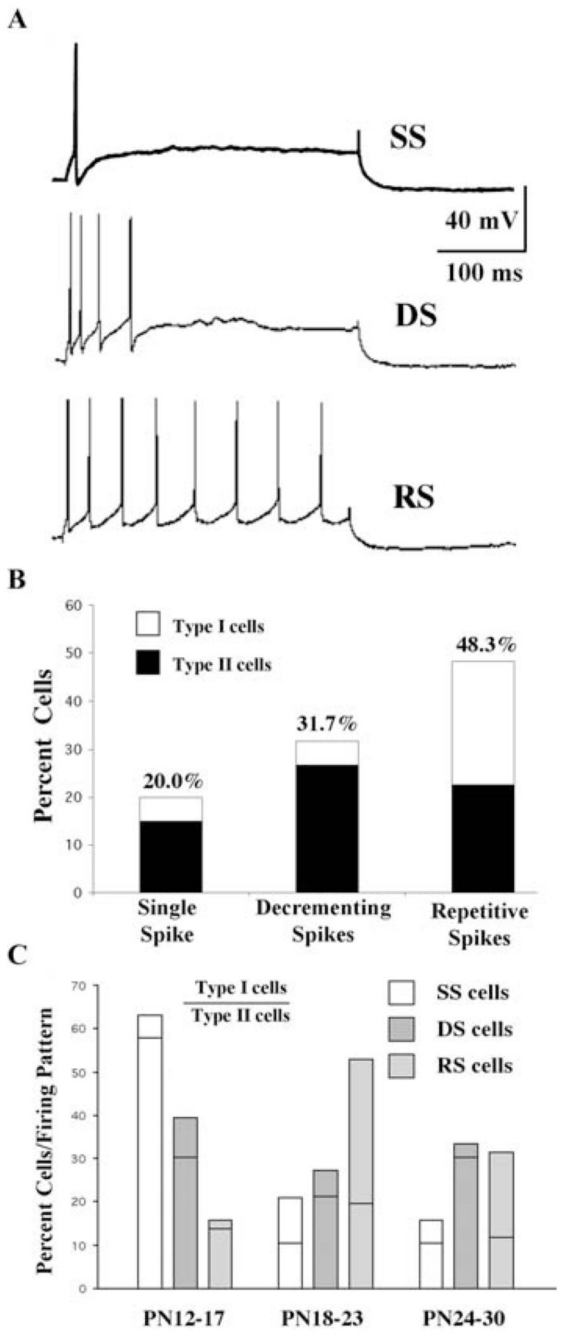


**Fig. 9. Developmental changes in depolarization-induced firing patterns in Pf cells**

(A) Examples of three types of firing patterns displayed by Pf cells: Single spike (SS) (top); decrementing or accommodating spikes (DS) (middle); and repetitive spikes (RS) (bottom). (B) Distribution of Type I and Type II cells with respect to the pattern of depolarization induced firing. (C) Distribution of Type I and Type II cells as a percentage grouped by firing pattern. The part of each bar above the horizontal line represents the contribution of Type I cells and that below the line indicates Type II cells. Single spike (SS, open bars); decrementing or accommodating spike (DS, hatched bars); repetitive spikes (RS, shaded bars).

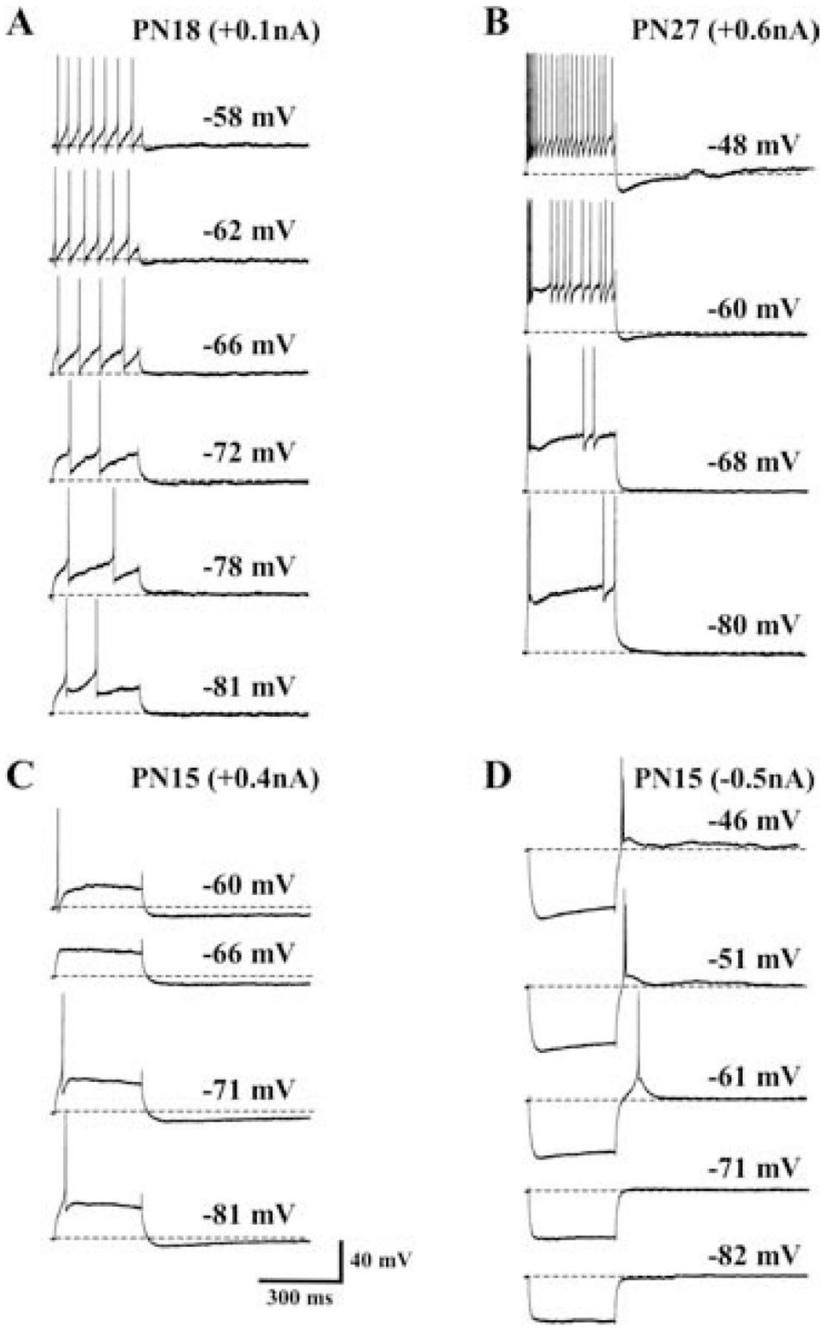


**Fig. 10. Voltage-dependence of cell firing in Pf cells**

(A) Voltage-dependent changes in the firing pattern of a representative Type I repetitively firing cell in response to a single depolarizing current step. Note the absence of any low threshold calcium spike (LTS), the increase in delay to first spike, and the apparent decrease in spike threshold as the membrane was hyperpolarized from −58 mV to −81 mV. (B) Voltage-dependent changes in firing pattern of a representative Type II cell. Note the slowing of cell firing as the membrane was hyperpolarized from −48 mV to −80 mV. The burst firing seen at the beginning of the step at −80 mV appears to be generated by a LTS-like response. (C) Response of a PN 15 single spike firing Pf cell to changes in membrane potential from −60 mV to −81 mV. Note the absence of cell firing at −66 mV and it exhibited only a single spike

when held at more hyperpolarized levels. The hyperpolarizing membrane rectification observed during the depolarizing current step appeared to be largely voltage-independent. (D) Voltage-dependence of the rebound response from a PN15 cell. Note the loss of the LTS-like response at −61 mV as the membrane potential was hyperpolarized to −81 mV. Calibration bars: vertical 40 mV; horizontal 300 ms.

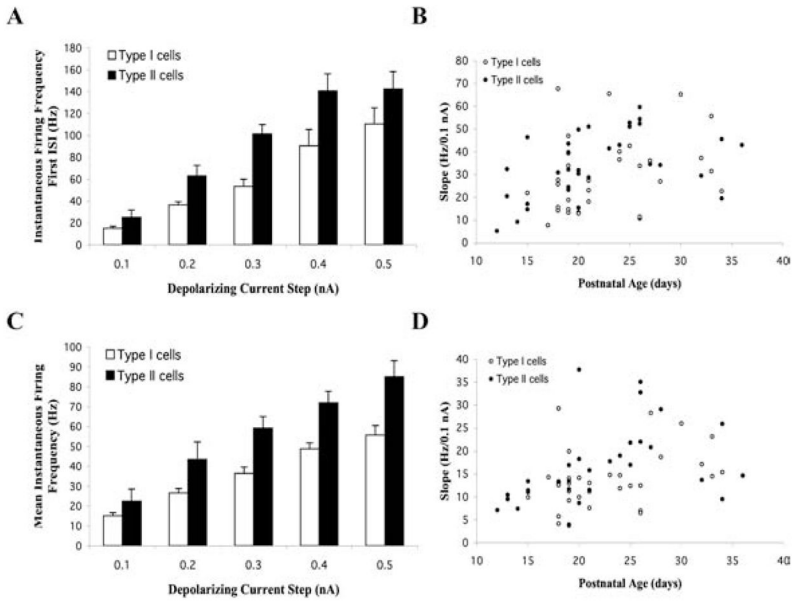


**Fig. 11. Developmental changes in the voltage-dependence of cell firing in Pf cells**

(A) Comparison of the instantaneous firing frequency for the initial interspike interval (ISI) plotted as a function of depolarizing current step in Type I and Type II cells (mean ± S.E.). (B) Mean slope of the instantaneous firing frequency of the first ISI in Type I and Type II cells plotted as a function of age. (C) Comparison of the mean instantaneous firing frequency for all ISIs plotted as a function of depolarizing current step in Type I and Type II cells. (D) Mean slope of the instantaneous firing frequency for all ISIs in Type I and Type II cells plotted as a function of age.

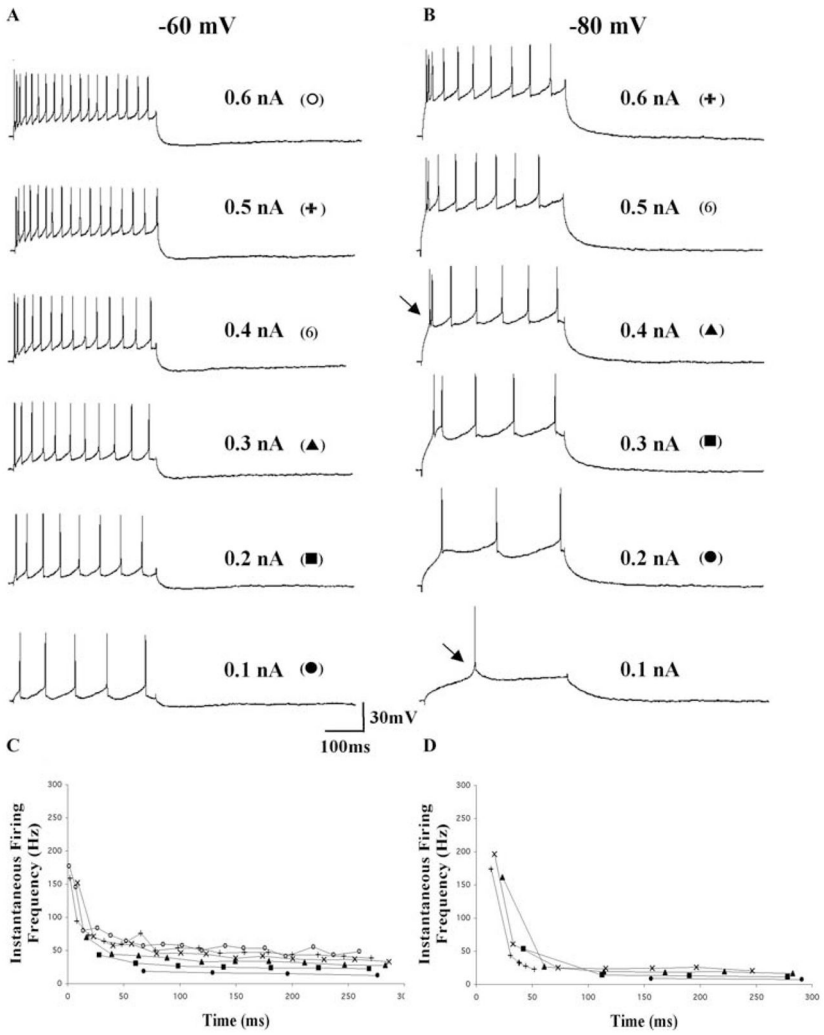


**Fig. 12. Voltage dependence of instantaneous firing frequency in a representative repetitively firing Pf cell**

(A, B) AP firing in response to increasing depolarizing current steps recorded at holding potentials of −60 mV (A) and −80 mV (B). (C, D) Plots of the instantaneous firing frequency taken from the recordings in A and B, respectively. This repetitively firing cell exhibited an initial burst (top arrow) during the first 50 ms of the depolarizing current steps followed by a sustained response regardless of the holding potential. Note the appearance of a LTS (bottom arrow) with a significant delay at −80 mV compared with −60 mV. This cell was a Type I PN 25 neuron. Calibration bars: vertical 30 mV; horizontal 100 ms.

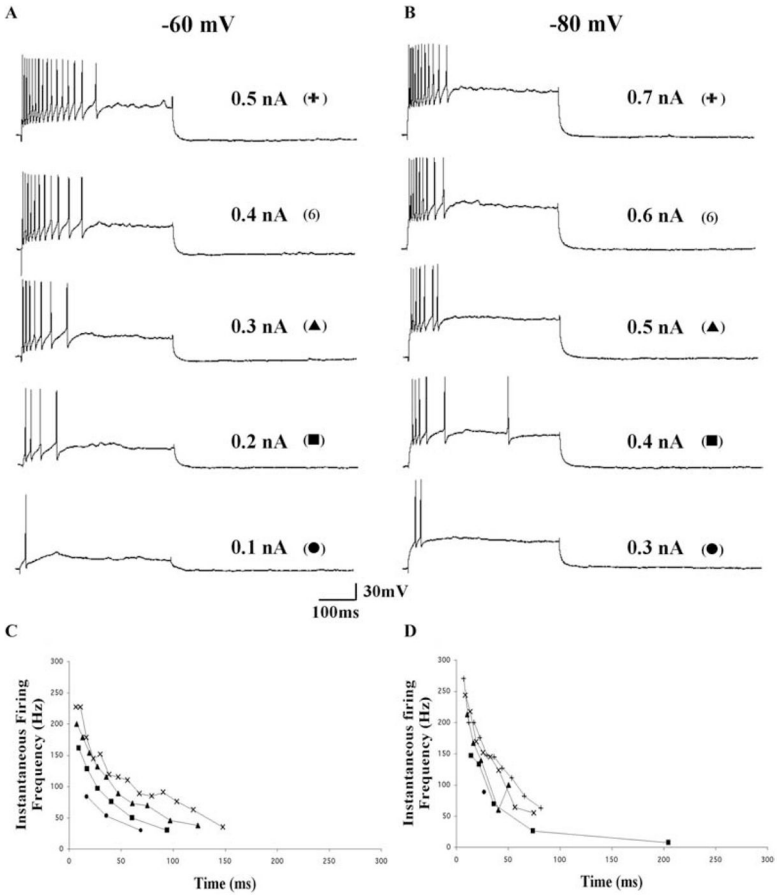


**Fig. 13. Voltage dependence of instantaneous firing frequency in a representative accommodating Pf cell**

(A, B) Action potential firing in response to increasing depolarizing current steps recorded at holding potentials of −60 mV (A) and −80 mV (B). (C, D) Plots of the instantaneous firing frequency taken from the recordings in A and B, respectively. Note the similar pattern of spike accommodation in this cell regardless of the holding potential. This cell was a Type II PN 25 neuron. Calibration bars: vertical 30 mV; horizontal 100 ms.

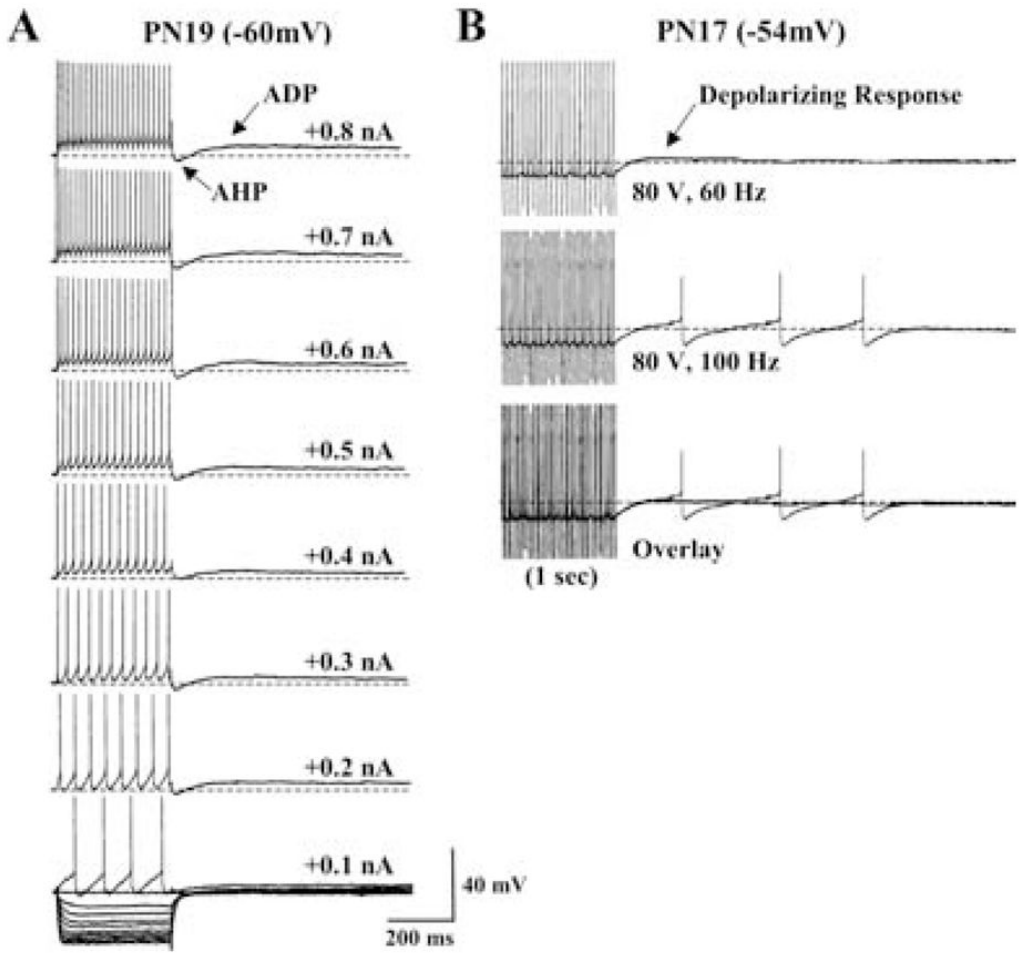


**Fig. 14. Depolarization induced ADPs following PPN-stimulation-evoked responses**

(A) A representative, repetitively firing Type I PN 19 Pf cell exhibiting a depolarization induced ADP. Note that the amplitude of the ADP increased slightly as a function of depolarizing current step but was not sufficient to induce cell spiking. (B) A Type I PN 17 Pf neuron in which stimulation of the PPN (80 V, 60 Hz, 1 sec) evoked a similar small amplitude depolarization that could induce action potential firing when stimulated at higher frequency (100 Hz). Calibration bars: vertical 40 mV; horizontal 200 ms.

**Table 1**

The intrinsic membrane properties of developing Pf cells

| | All cells | | | Type I cells | | | Type II cells | | |
|---|---|---|---|---|---|---|---|---|---|
| | **RMP (mV)** | **Rin (MΩ)** | **TC (ms)** | **RMP (mV)** | **Rin (MΩ)** | **TC (ms)** | **RMP (mV)** | **Rin (MΩ)** | **TC (ms)** |
| All cells | −55.2 ± 0.5 (172) | 107.8 ± 4.3 (152) | 9.3 ± 0.5 (136) | −55.5 ± 0.8 (49) | 121.3 ± 8.4 (45) | 11.0 ± 0.8 (42) | −55.0 ± 0.6 (123) | 102.2 ± 5.0 (107)# | 8.5 ± 0.5 (94)# |
| PN 12–17 | −55.8 ± 1.0 (45) | 105.3 ±10.2 (42) | 11.3 ± 1.2 (28) | −56.4 ± 2.3 (7) | 116.0 ± 20.8 (7) | 10.9 ± 2.1 (2) | −55.7 ± 1.1 (38) | 103.2 ± 11.5 (35) | 11.3 ± 1.3 (26) |
| PN 18–23 | −53.5 ± 0.8 (64) | 112.7 ±7.5 (55) | 8.4 ± 0.7 (54) | −54.4 ±1.4 (21) | 126.5 ± 16.4 (20) | 10.5 ± 1.3 (20) | −53.0 ± 1.1 (43) | 104.8 ± 7.0 (35) | 7.1 ± 0.6 (34)* |
| PN 24–30 | −58.0 ± 1.0 (42)†† | 103.1 ±5.9 (37) | 8.6 ± 0.8 (36) | −58.4 ± 1.0 (14) † | 118.8 ± 8.3 (13) | 11.6 ± 1.2 (14) | −57.7 ± 1.4 (28)†† | 95.4 ± 7.4 (24) | 6.8 ± 0.8 (22)** |

*$P < 0.05$,

**$P < 0.01$ compared with PN 12–17;

†$P < 0.05$,

††$P < 0.01$ compared with PN 18–23;

#$P < 0.05$ compared with Type I cells).

**Table 2**

The AP properties of developing Pf cells

| | All cells | | | Type I cells | | | Type II cells | | |
|---|---|---|---|---|---|---|---|---|---|
| | **AP threshold (mV)** | **AP amplitude (mV)** | **AP duration (ms)** | **AP threshold (mV)** | **AP amplitude (mV)** | **AP duration (ms)** | **AP threshold (mV)** | **AP Amplitude (mV)** | **AP duration (ms)** |
| All cells | −42.7 ±0.6 (99) | 47.3 ±0.9 (97) | 0.93 ± 0.04 (96) | −42.8 ±0.9 (41) | 48.6 ± 1.4 (40) | 0.85 ± 0.06 (40) | −42.6 ± 0.9 (58) | 46.3 ± 1.1 (57) | 0.99 ± 0.06 (56) |
| PN 12–17 | −41.9 ± 1.3 (32) | 44.2 ± 1.6 (31) | 1.31 ± 0.07 (31) | −42.1 ± 1.7 (14) | 47.2 ± 2.3 (14) | 1.09 ± 0.09 (13) | −41.8 ± 1.9 (18) | 41.7 ± 2.0 (17) | 1.47 ± 0.09 (18)# |
| PN 18–23 | −41.8 ± 1.0 (31) | 49.1 ± 1.3 (31) | 0.79 ± 0.05 (31)** | −42.8 ± 1.4 (14) | 48.9 ± 2.2 (14) | 0.73 ± 0.09 (14)* | −41.1 ± 1.4 (17) | 49.2 ± 1.6 (17) | 0.83 ± 0.05 (17)** |
| PN 24–30 | −45.3 ± 1.3 (23) | 50.3 ± 1.9 (22)* | 0.69 ± 0.05 (21)** | −43.6 ± 2.3 (10) | 48.6 ± 4.1 (9) | 0.68 ± 0.11 (10)* | −46.7 ± 1.6 (13) | 51.5 ± 1.7 (13)* | 0.68 ± 0.03 (11)** |

*$P < 0.05$,

**$P < 0.01$ compared with PN 12–17;

#$P < 0.05$ compared with Type I cells).